

Finite Element Analysis of the Heat Transfer in a Copper Mould
during Continuous Casting of Steel Slabs

14 May 2005

D. Hodgson, Sami Vapalahti, and B.G. Thomas

Department of Mechanical and Industrial Engineering
University of Illinois at Urbana-Champaign
Urbana, IL 61801
bgthomas@uiuc.edu

Abstract

To calibrate the CON1D model for accurate simulation of mold temperature and heat flux in a thin-slab casting mold, 3-dimensional heat transfer computations were performed using ANSYS and used to find the offset distance for CON1D. The CON1D model was found to produce accurate simulations everywhere across the wideface, so long as the mold thickness is set to 33.4mm and the thermocouple positions are offset by 1.8mm (moving thermocouples computationally from 14mm to 12.2mm from the hot face). Thermocouple temperatures drop greatly if there is any contact problem attaching them (~10 °C drop for just a contact resistance equivalent to 0.01mm air gap)

Introduction

Copper continuous casting moulds are used heavily in steel production to produce high quality steel sheets from molten steel. These sheets are produced by pouring the molten steel into the mould which removes enough heat to solidify the outer layers into a solid steel shell. The partially solid steel is removed at a constant rate, allowing the steel to be continuously poured into the mould, finishing solidification further along the casting system. Due to the high temperatures involved in the process, the copper is cooled by pumping cooling water through slots within the mould. This is monitored by thermocouples placed at regular intervals throughout the mould.

The thermocouples are there to note any unexpected temperature rises, which could be indications of unusual cooling flow, leading to damage to the copper. This is important as any damage to the copper could create cracks, which if they were allowed to propagate to the cooling slots, cause catastrophic failure. The necessary safety and working life considerations mean that the thermocouples are set back from the hot face of the mould. It is therefore necessary to have an understanding of the temperature distribution and heat flux within the mould to know the relationship between the hot face temperature and the measured temperature at the thermocouples.

This is initially an investigation into the temperature distribution with a small, 5mm thick section.

This was followed by investigating the effect of the thermocouple placement holes on the temperature distribution as well as the cooling effect of the thermocouple wire by conducting heat away from the mould. This cooling effect could lead to inaccurate readings from the thermocouple and a slightly different temperature distribution through the mould. As before the model will be a 5mm section of the mould.

This data developed from these simulations can be used to find what is known as offset values for this mould. These offset values are used to allow a simple simulation, in this case CON1D¹ which is a FORTRAN simulation, to be used to predict this more complex mould. These offset values will be reasonably constant and would be specific to this mould. To help find these offset values the simulation will be run at different depths the temperature profile investigated. The depths looked at will be 800mm, 400mm and 110mm below the meniscus

To allow easier referencing the initial investigation will be referred to as Case 1 at 800mm below the meniscus. The following investigation into the effect of the thermocouple hole and the cooling effect of the thermocouple wire will be referred to as Case 2 and 3 respectively, both at 800mm. The simulations at different depths will be Case 2 for 400mm and 110mm. A fourth case will also be looked at investigating the effect of the mould thickness.

The final investigation of this study will be to create a 3-D simulation of the mould expanding the domain to a 130mm section rather than the thin section used previously. This will allow the inclusion of a varying heat flux in relation to the depth. As the steel cools the amount of heat being absorbed by the mould reduces. In the case of the casting mould this means that the heat flux is at a maximum at the meniscus and reduces as the depth below the meniscus increases. This larger model will investigate the interaction of this varying heat flux on the temperature profile within the mould.

Model Description

The equation being solved is the 3-D heat conduction equation shown below:

$$\frac{\partial}{\partial x} k \frac{\partial T}{\partial x} + \frac{\partial}{\partial y} k \frac{\partial T}{\partial y} + \frac{\partial}{\partial z} k \frac{\partial T}{\partial z} = 0$$

This will be solved using ANSYS 8.0² for the first simple domains of an Algoma mould and the domain is described below. The final simulation of a 3-D section will be modelled using FEMLAB³ as this program's license allows a larger number of nodes and elements.

Domain

The copper mould being simulated is shown below. Figure 1 shows a schematic top view of the mould and Figure 2 shows a close up of horizontal section.

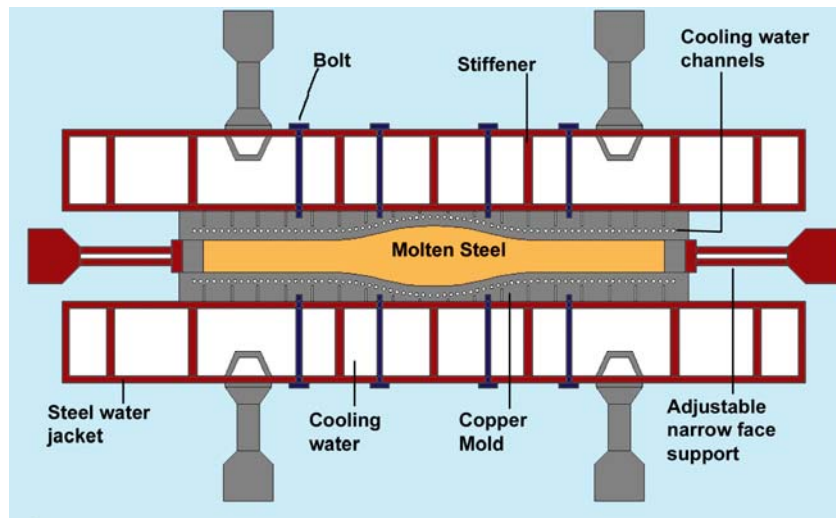
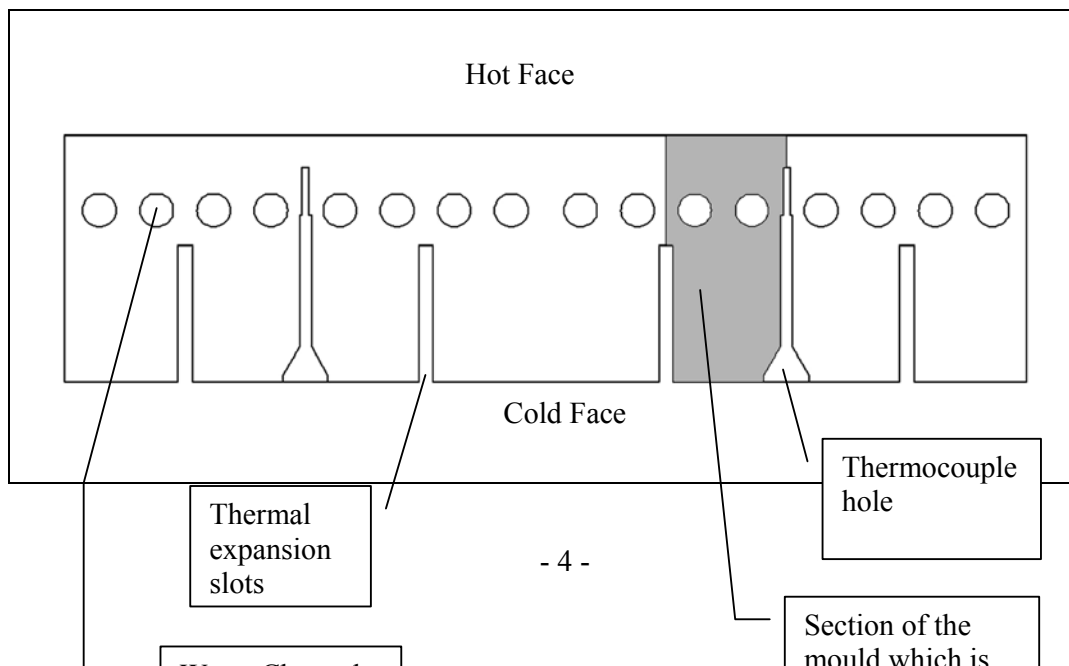


Figure 1: Schematic top view of mould



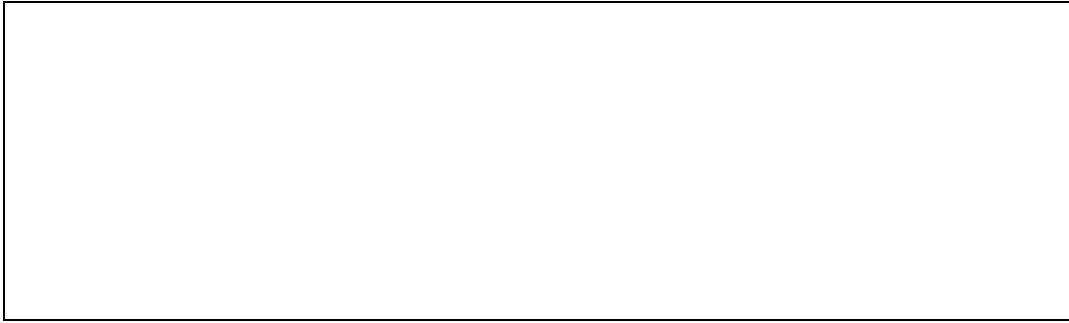


Figure 2: Close up of horizontal section

In Figure 2 the circular pipes are the cooling water tubes rather than the rectangular slots common in mould design. The rectangular slots are structural expansion slots and therefore have negligible heat transfer effects. These expansion slots are designed to allow the thermal expansion of the hot face during operation to lessen constraint caused by the cold side thereby lowering operational stresses and residual stress. It can be seen that there is slightly greater spacing between the bored holes that straddle the thermocouple holes to allow them to fit.

In the first case a simplified domain was used, this domain was reduced using symmetry. The domain is shown in Figure 3; the position of the thermocouple is indicated. This domain was used in Case 1. This case does not include the thermocouple hole to investigate its effect on the temperature distribution.

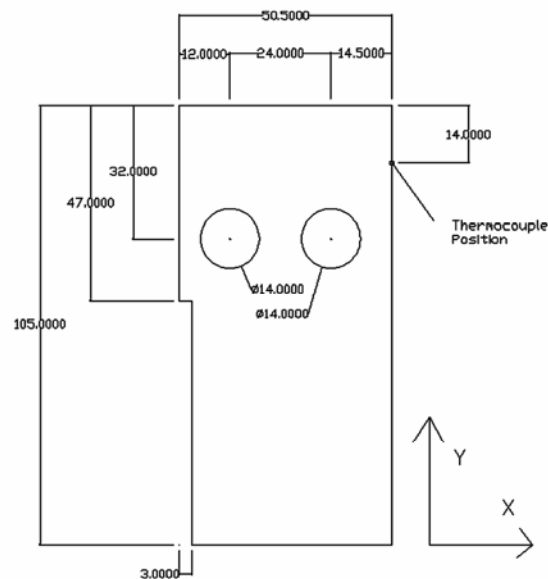


Figure 3: Simplified Domain, all units in mm

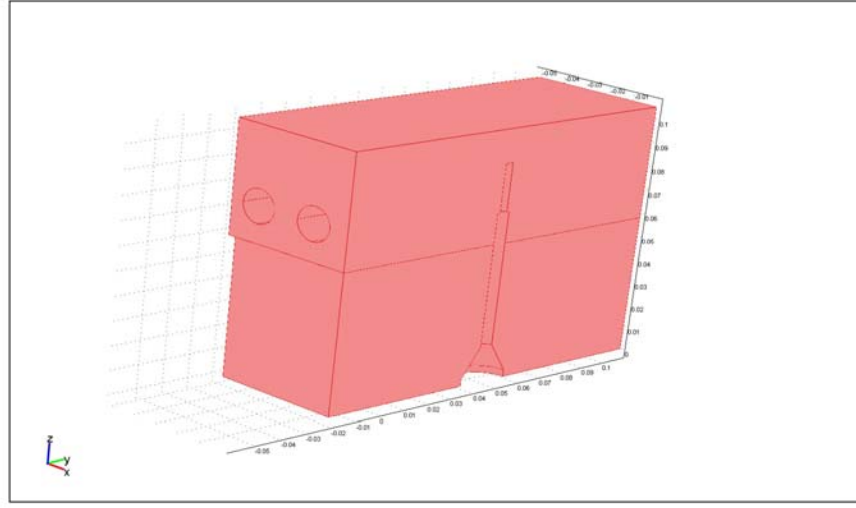


Figure 5: Domain of Case 5 simulation, expanded domain to a depth of 130mm

Boundary Conditions

The finite-element model was developed to calculate the temperature in a typical thin slab casting funnel mould during steady state operating conditions. The funnel measures 800mm wide at the top with a depth of 40mm at the mould top and tapers down to 800mm wide and 8mm deep at the bottom. However this was likely to have a negligible effect on the mould temperature and thermocouple temperature because the distance of the cooling tubes and thermocouple from the hot face remains constant throughout the mould.

The domain considers a section 5mm deep at a specific depth of 110mm, 400mm and 800mm below the meniscus of the molten steel. The sections are shallow, 5mm deep, to allow the assumption that the heat flux at the hot face remains constant; however the simulation was still a 3-D model to be accurate and to allow easy development of the domain to a bigger section. Table 1 shows the Simulation Conditions used in the first four cases. These conditions were taken from the results of a CON1D simulation:

Table 1: Simulation Conditions

Boundary Condition in all Cases				
Thermal conductivity of copper		372 W m ⁻¹ K ⁻¹		
Distance of thermocouple from hot face		14mm		
Remaining faces of model		Perfectly insulated		
Water Velocity in bored holes		8.7 m/s		
Boundary Conditions at Individual Depths				
Depth below meniscus (mm)		110	400	800
Heat Flux (MW m ⁻²)		3.18	2.201	1.704
Water tube heat transfer coefficient (kW m ⁻² K ⁻²)		32.4412	34.6691	35.7748
Water temperature (°C)		21.31	25.00	28.31

Note that the heat transfer coefficient varies with position in the mould. The coefficient increases as the depth increases due to heating of the water.

The results of these simulations will be divided into five different cases:

- Case 1) No thermocouple hole present in domain.
- Case 2) The thermocouple hole included in domain though the cooling effect of the thermocouple wire was not included.
- Case 3) Both the thermocouple hole and the cooling effect are modelled in the domain.
- Case 4) Case 2 with 65-mm thick mould section, (vs. 105 mm mould section) smaller domain.
- Case 5) Similar dimensions to previous cases however domain has been expanded to a depth of 130mm.

Table 2 and Figure 6 show the boundary conditions used in Case 5. The heat transfer coefficient and water temperature are averages of CON1D data. This was done to reduce computation time. The heat flux data was inserted into the simulation and is shown in Figure 6. This data is made up of points which were used to interpolate intermediate heat flux values. This interpolation is achieved within FEMLAB using a piecewise cubic method.

Table 2: The boundary conditions used in Case 5

Boundary conditions for Case 5	
Water tube heat transfer coefficient ($\text{kW m}^{-2}\text{K}^{-2}$)	34712.16
Water temperature($^{\circ}\text{C}$)	25.50347

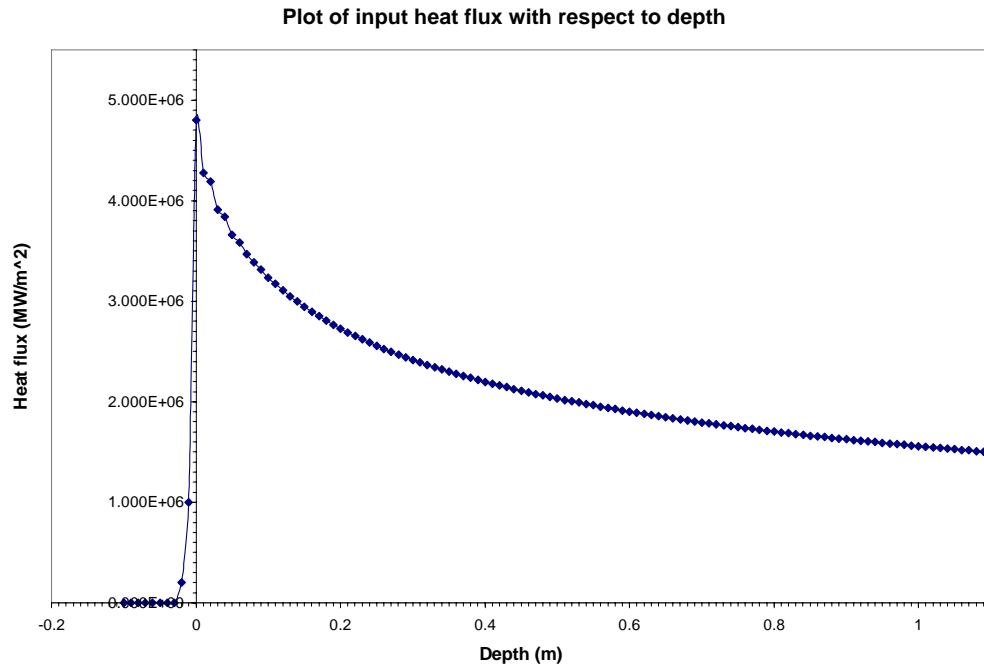


Figure 6: Plot showing the change of heat flux as depth increases. This is the data used for Case 5

The first three cases were investigated at 800mm to allow comparison and investigate the effect of the thermocouple on the temperature distribution. From these results it was decided to compare Case 2 at various depths, 110mm and 400mm to investigate how the results differ from those calculated using CON1D. These results can be used to calculate off-set values to allow the faster running CON1D simulation to predict temperatures for the mould.

The finite-element simulation for Case1 was solved using ANSYS 8.0 on a Dell Precision 450N desktop computer. The mesh was made of 20 node brick elements in a 3-D analysis containing 15777 Nodes and 9356 Elements and was executed quickly. A view of the mesh used is shown in Figure 7

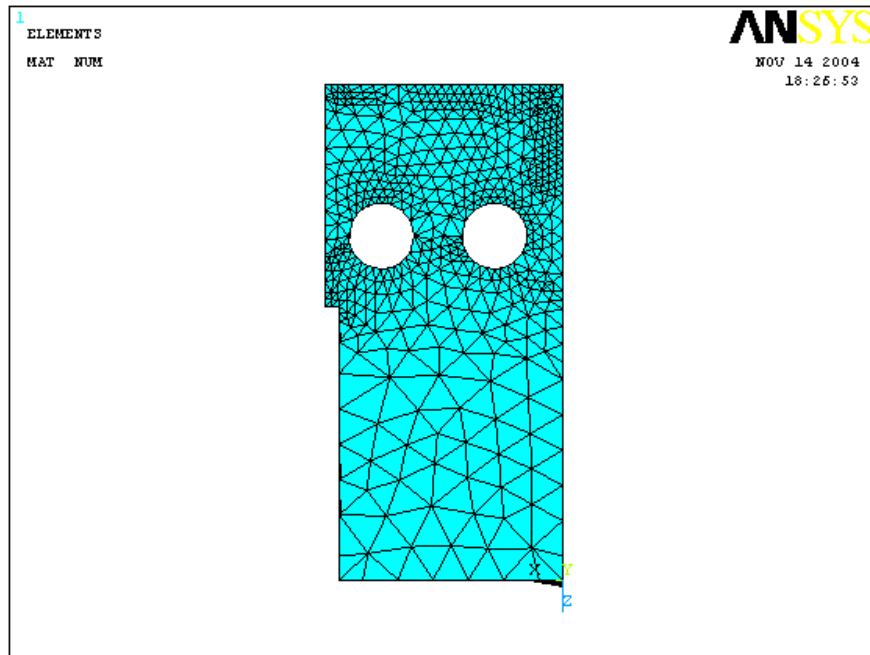


Figure 7: Mesh of Case 1, containing 9931 nodes and 17434 elements

Notice that the mesh has been refined in the vicinity of the thermocouple; this creates ~20 elements from the hot face to the thermocouple.

The finite-element simulation for Cases 2 and 3 was solved using ANSYS 8.0 on a Dell Precision 450N desktop computer. The mesh was again made of 20 node brick elements in a 3-D analysis containing 9931 Nodes and 17434 Elements and was executed quickly. As in the previous mesh, refinement was increased around the thermocouple hole to increase the accuracy of the results. A view of the mesh used is shown in Figure 8

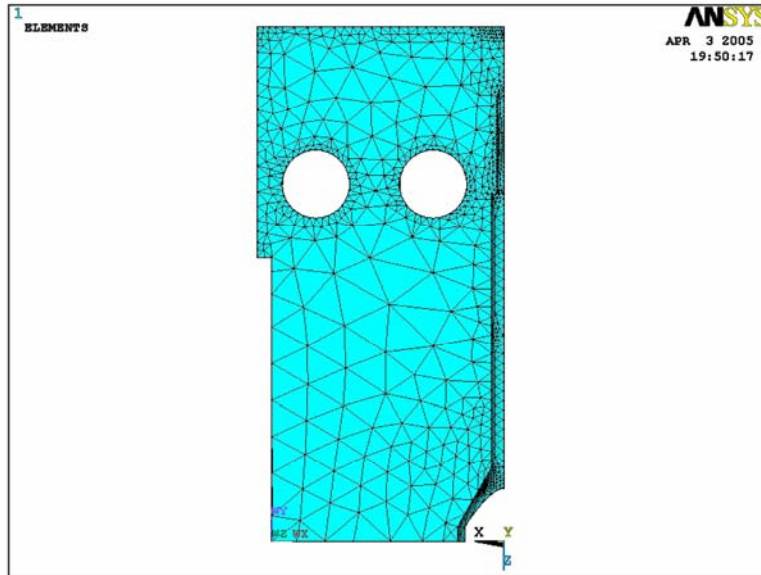


Figure 8: View of mesh used for Cases 2 and 3, containing 3140 Nodes and 12926 Elements

The finite-element simulation of Case 5, the large 3-D section, was solved using FEMLAB 3.1 on a Dell Inspiron 5150 laptop. The mesh was made 72345 elements and took about 125 seconds to execute. Below in Figure 9 is a view of the mesh.

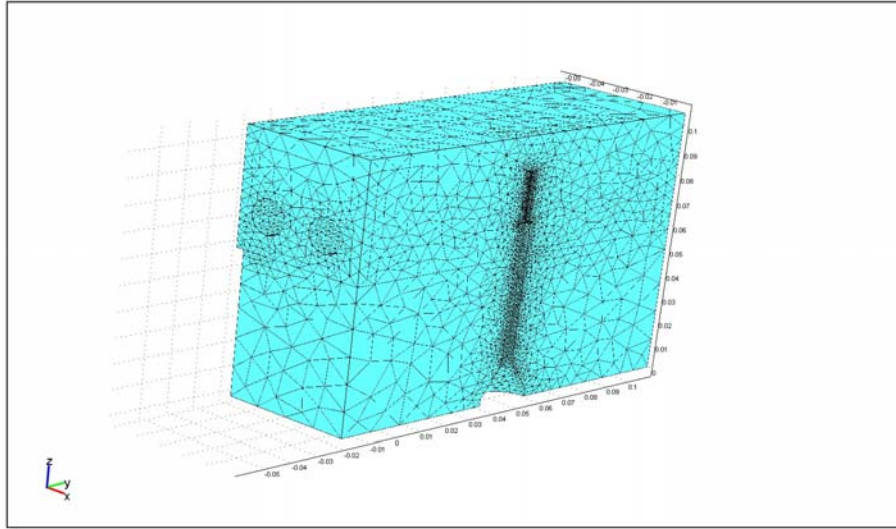


Figure 9: View of the mesh for Case 5, large 3-D section

Calculating the Cooling Effect of the Thermocouple Wire

The cooling effect was investigated in Case 3 using an iterative method based on a wire divided into two sections with different conditions along each section. In Figure 10 a diagram of the wire model is shown.

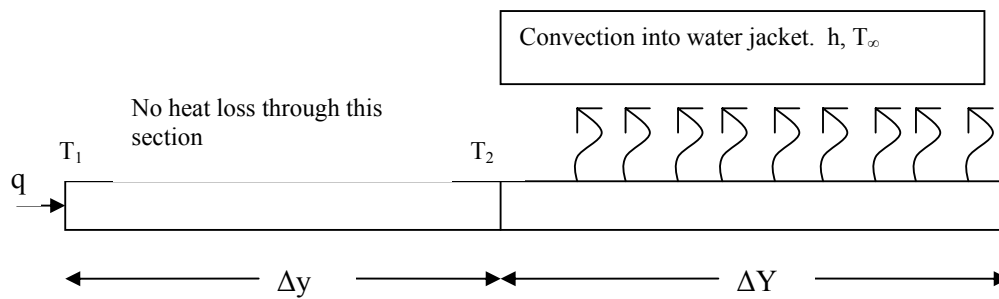


Figure 10: Diagram of the wire model used to calculate the cooling effect

The first section was treated as a conductive wire with a fixed temperature at one end. It was assumed that no heat loss occurred from the surface as the ambient

temperature would be similar to the wire due to the air being heated by the surrounding mould. This is connected to the second section where heat loss occurs by convection. All the heat transported down the wire is assumed to be lost through this section. The iteration is necessary as the initial temperature difference in the first section is estimated. Repeated calculations are made to refine this temperature difference. No conduction along the wire in the convective section was calculated to simplify the process. Below is an example calculation with the conditions shown in Table 3.

Table 3: Conditions used in iterative calculation

T_1	139°C
T_2	34°C
T_∞	28.31°C
h	20000 Wm ⁻² K ⁻¹
k	22 Wm ⁻¹ K ⁻¹
Δy	0.103m
ΔY	0.2m
Diameter, D	0.003m
Area, A	$7.0686 \times 10^{-6} \text{ m}^2$
Perimeter area in convective section, P	0.001884 m ²

The purpose of this iterative calculation is to solve the following with respect to T_2 forcing heat fluxes to match

$$q = \frac{k_{\text{con}} A (T_1 - T_2)}{\Delta y} = hP(T_2 - T_\infty)$$

Calculation : Conduction along first section

$$q = \frac{(k \times (T_1 - T_2) \times A)}{dy} = \frac{(22 \times 105 \times 7.0686 \times 10^{-6})}{0.103}$$

$$q = 0.158529W$$

Calculation : Heat loss through second section to find necessary temperature difference

$$q = h \times (T_2^{\text{new}} - T_\infty) \times P$$

$$0.158529 = 20000 \times (T_2^{\text{new}} - 28.31) \times 0.001884$$

from this T_2^{new} can be found

$$T_2^{\text{new}} = 28.3142^\circ\text{C}$$

From this new T_2 value a new $(T_1 - T_2)$ is found, 110.686°C. This means a new

q needs to be calculated and the process is repeated. Eventually this settles on a value for T_2 of 28.31443°C and the amount of heat transported down the wire is 0.167112W.

The simplification of the calculation by not modelling the conduction along the wire in the water cooled section has the added benefit of causing the value to be an upper bound. In reality the heat loss down the wire is less than calculated as the temperature at the end of the first section would be higher leading to less heat conducted down the wire.

This method assumes that the wire end has perfect contact with the bottom of the hole. If there is thermal contact resistance then the temperature at the end of wire, the temperature that is actually measured drops significantly due to the insulating effect of air. The actual situation at thermocouple ends needs to be investigated to ensure accuracy of the readings. The effect of an air gap was investigated by recalculating the previous results with the extra thermal resistance of an air gap. Different sizes of air gap were looked at comparing the new amount of heat conducted away and the temperature that would exist at the thermocouple tip. Throughout this investigation the previous conditions were used with the following additions, Table 4. The results are shown below in Table 5 and Figure 11.

Table 4: Extra to investigate air gap effect

k of air (W/mK)	0.024
Resistance of wire (K/W)	662.34

Table 5: Results of air gap investigation

Air gap thickness (m)	Thermal resistance of air (K/W)	q conducted through wire (W)	T_2 (°C)	Temperature at thermocouple bead (°C)
0	0	0.167112505	28.31	139
0.00001	58.94627522	0.153455964	28.31	129.9543425
0.0001	589.4627522	0.088422486	28.31	86.87823801
0.00025	1473.65688	0.051820554	28.31	62.63428414
0.0005	2947.313761	0.030664752	28.31	48.62135479
0.001	5894.627522	0.016881207	28.31	39.49157363

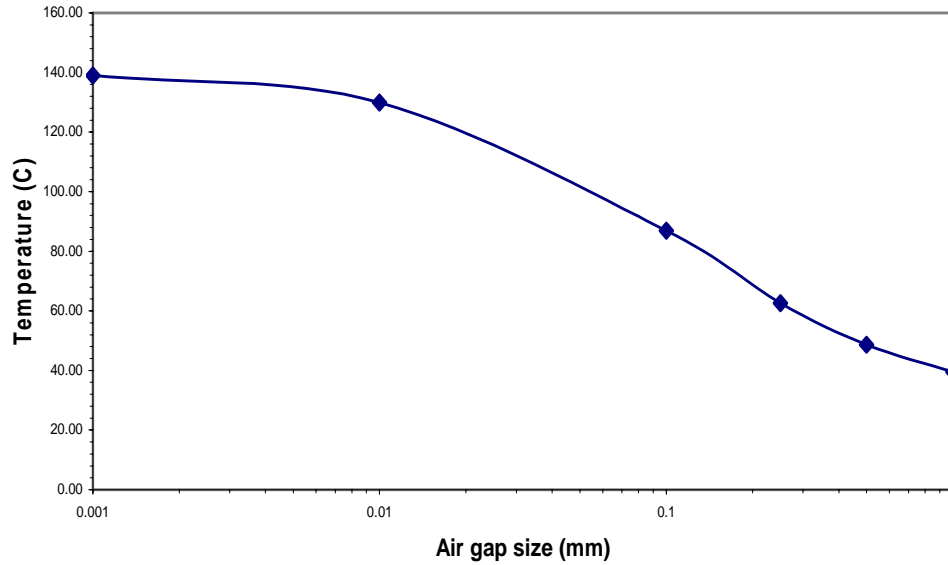


Figure 11: Plot of thermocouple bead temperature compared to the size of the air gap between the thermocouple and base of the probe hole

As can be seen the effect of a relatively small gap, 0.5 mm, is large reducing the amount of heat that is conducted away by over a fifth and reducing the temperature reading at the thermocouple bead by $\sim 90^{\circ}\text{C}$. These results show that the contact situation of the thermocouples within the mould is very important and care has to be taken to insure full contact.

The heat loss of a perfect thermocouple contact is added to Case 2 to create Case 3, investigating its effect on the temperature profile. This will be compared with the temperature profile of Case 2, without the heat loss due to the wire. Both these simulations will be compared with Case 1 to check for accuracy and to investigate whether the mould can be simulated more simply.

This method was also applied to the other depths to see if more heat would be removed by the wire at higher temperatures. T_2 appears to settle at roughly the same value as the lower depth of 800mm, 28.3°C . This indicates that the different amounts of heat are removed varying from 0.311186W to 0.167112W. These larger values are still small enough to be negligible from the simulations.

Results

Case 1 at 800mm below the meniscus

The temperature profile of Case 1 is shown in Figure 12. Figures 13 and 14 are alternative plots of the same data.

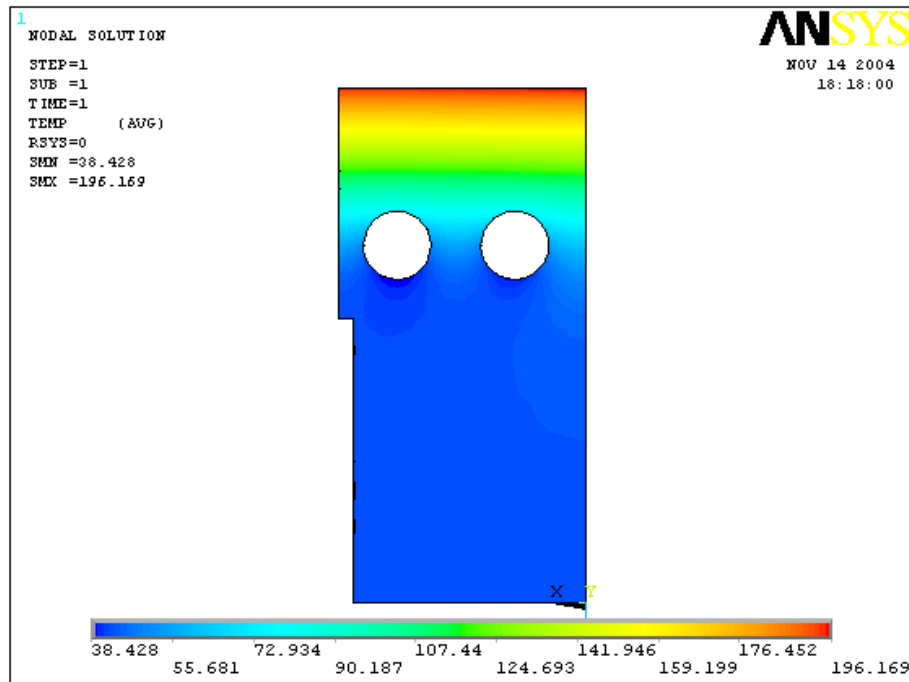


Figure 12: Temperature profile of Case 1 at 800mm

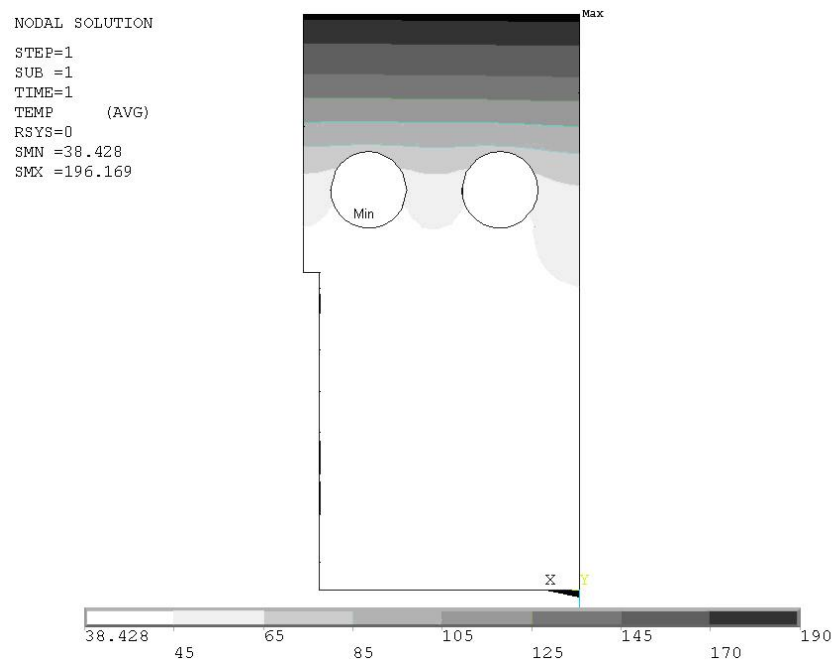


Figure 13: Greyscale of Temperature plot of Case 1 at 800mm

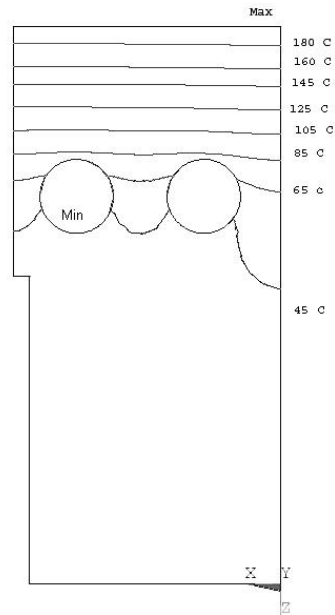


Figure 14: Isoline Plot of Temperature of Case 1 at 800mm

The maximum temperature, found to be 196.2°C , is at the hot face and the lowest, 38.4°C , was found on the cooling tube wall. Figure 15 is a graph showing the temperature drop along the edge where the thermocouple position is estimated, 14mm from the hot face.

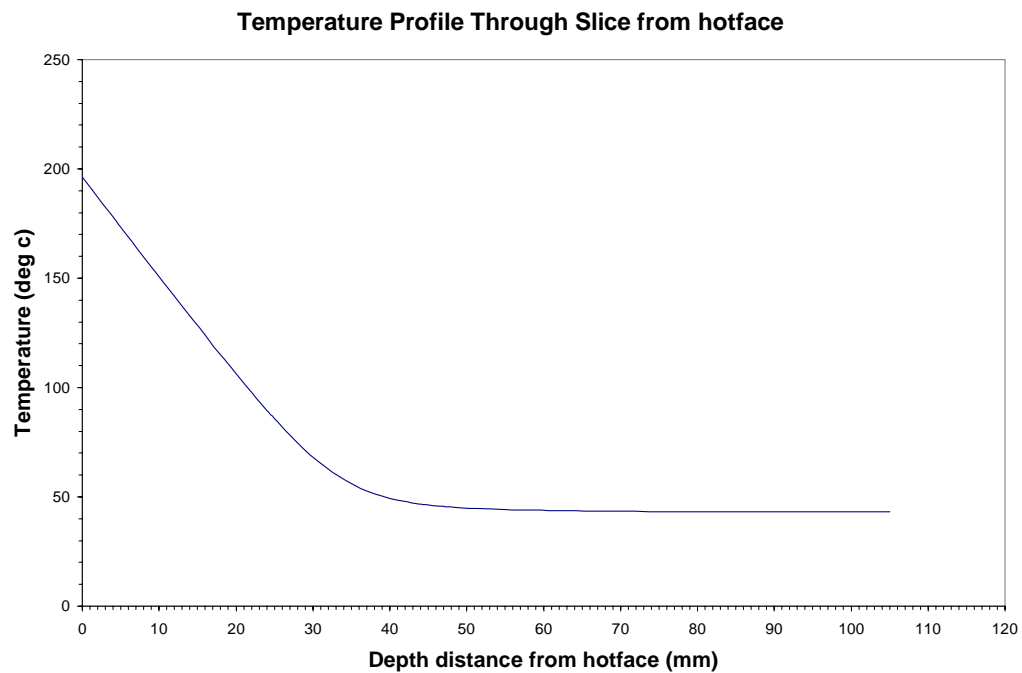


Figure 15: Temperature drop from hot face

The thermocouple temperature can be interpolated from the data using a linear method and is found to be 132.7°C. As can be seen the rate of temperature change reduces greatly once past the cooling tubes at 58mm reaching a reasonably constant temperature of 43°C.

Below in Figure 16 is a comparison of the temperature profiles from the hot face to the cooling tubes depth at different positions along the model. As can be seen the temperature profiles do not alter hugely along the model. The positions of these paths is shown in Figure 17

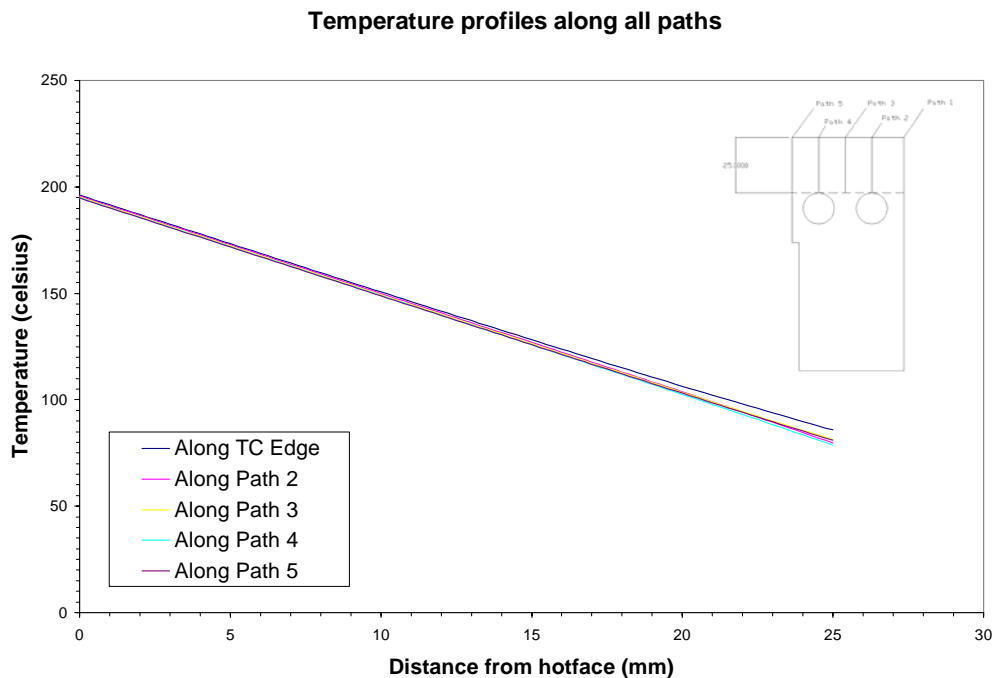


Figure 16: Temperature profiles at different positions along model in Case 1 at 800mm

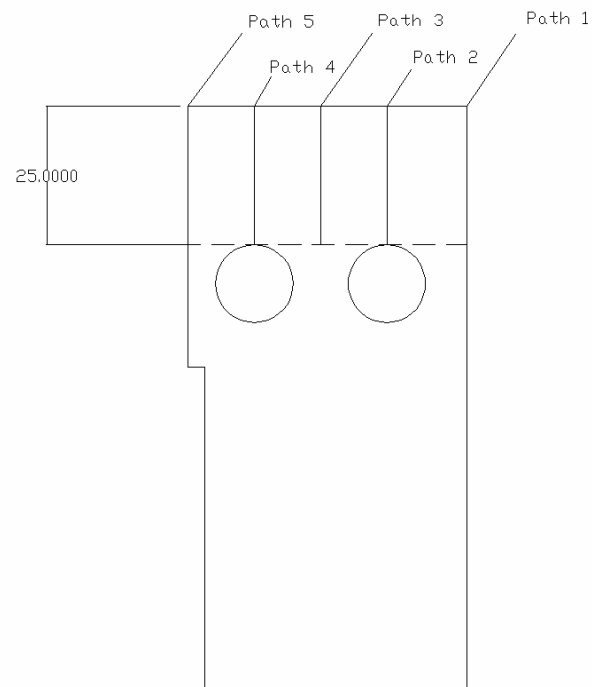


Figure 17: Position of paths on model in Case 1 at 800mm

Case 2 at 800mm below the meniscus

Below, Figure 18 is the temperature profile of Case 2 at 800mm below the meniscus, where the thermocouple hole is present however the heat loss due to the wire is not included.

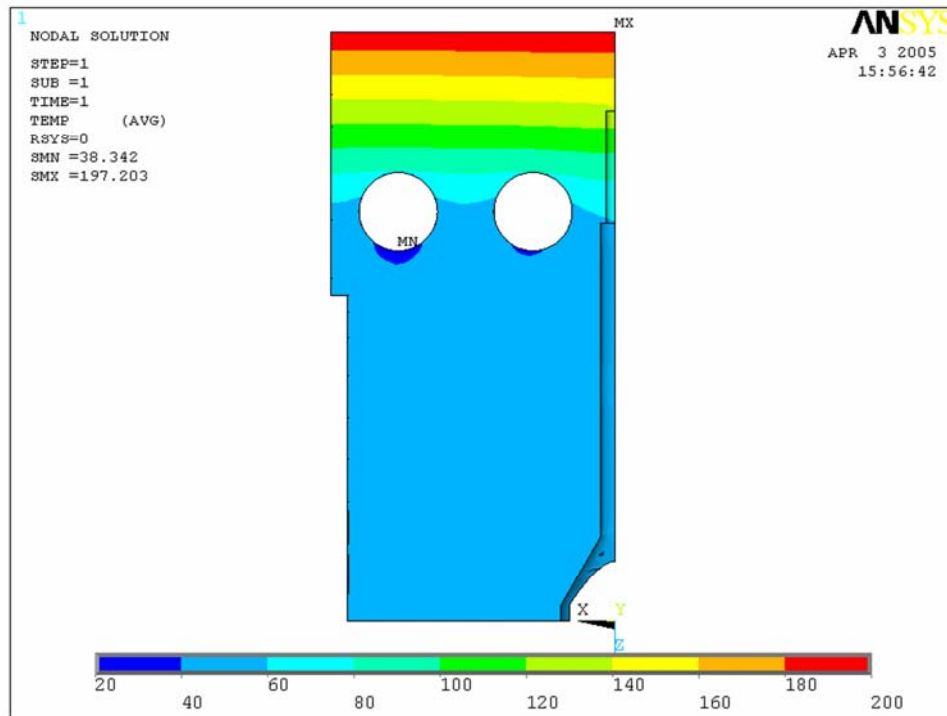


Figure 18: Temperature profile of Case 2 at 800mm

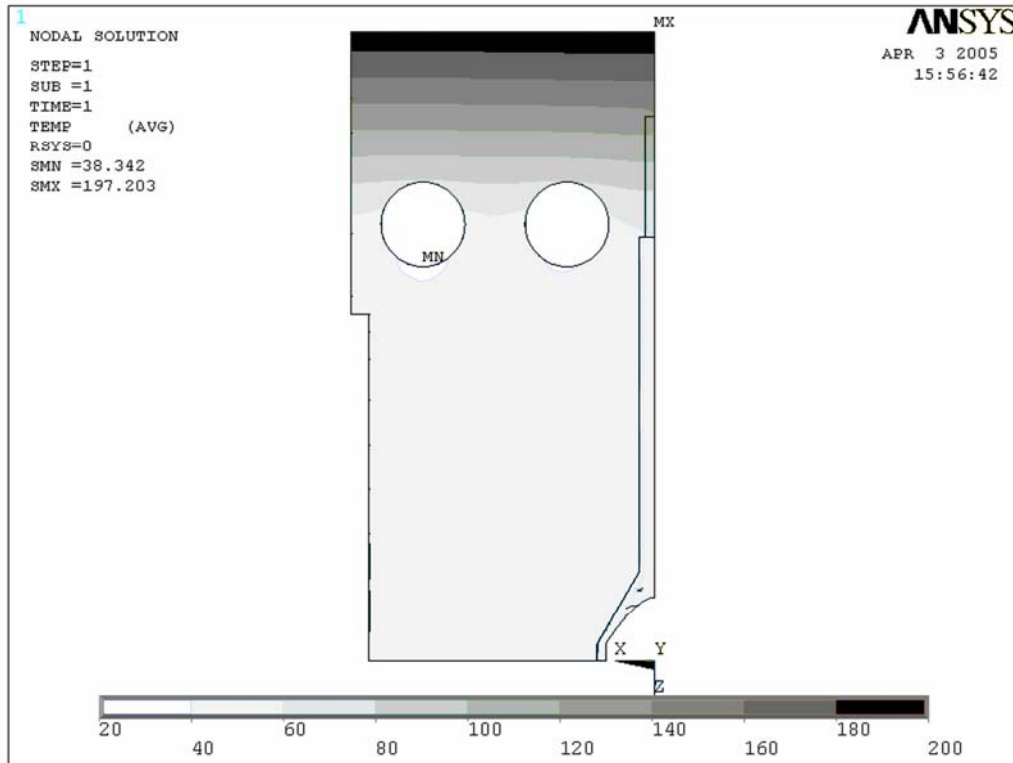


Figure 19: Greyscale of Temperature plot of Case 2 at 800mm

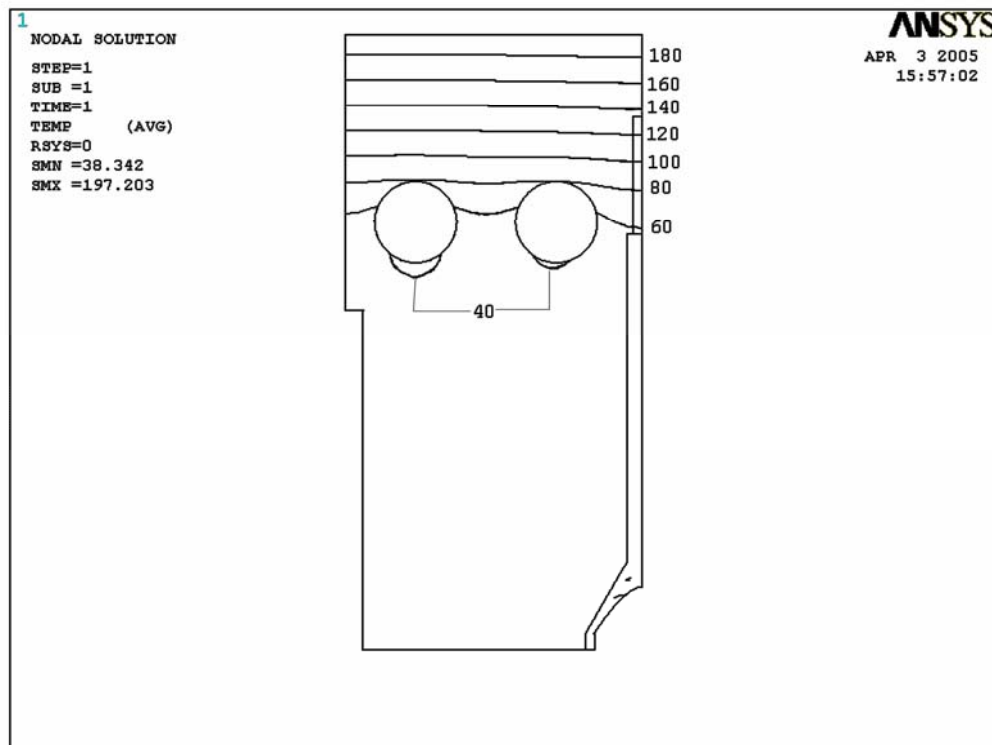


Figure 20: Isoline Plot of Temperature of Case 2 at 800mm

The maximum temperature found was 197.203°C; this is at the hot face and is in a similar position as Case 1 at 800mm. The minimum temperature was found to be 38.342°C and placed on the surface of the left cooling tube. This is also similar to Case 1 at 800mm.

The figures shown above do not give the best representation of the temperature within the section, below is Figure 21 showing the temperature profile of the top surface of the domain.

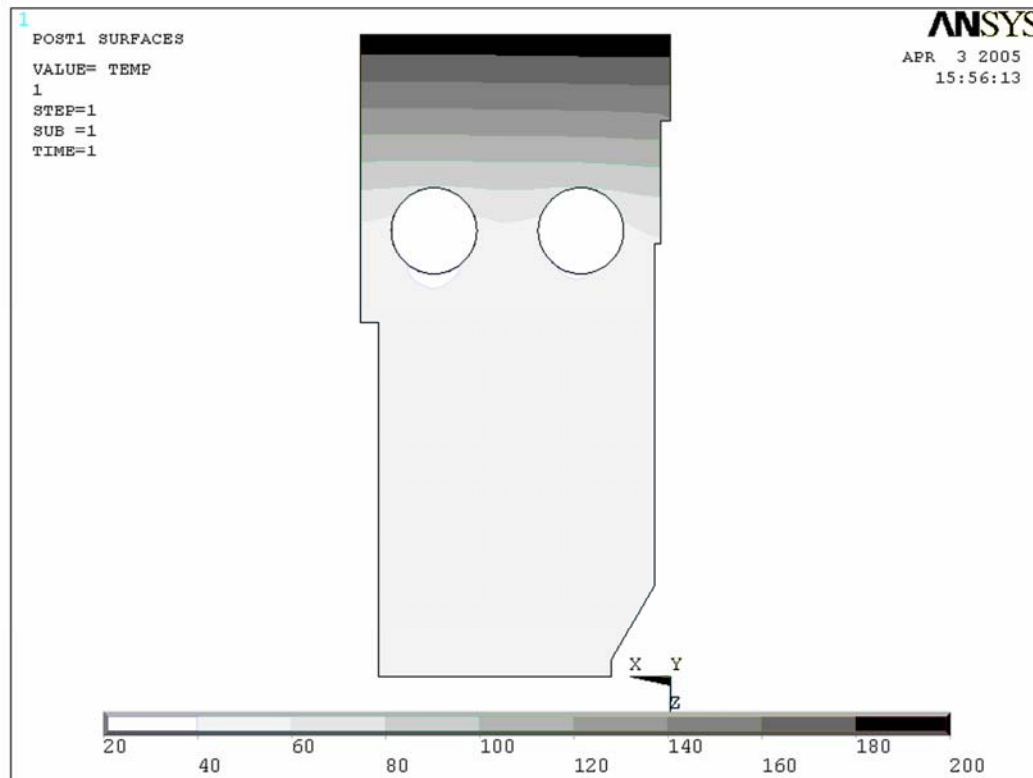


Figure 21: Temperature profile through centre of section in Case 2 at 800mm

Case 3 at 800mm below the meniscus

Below is the temperature profile of Run 3. In this case the model contains the thermocouple hole and the cooling effect of the thermocouple wire. The profile is presented in three different forms as before, Figure 22, 23 and 24

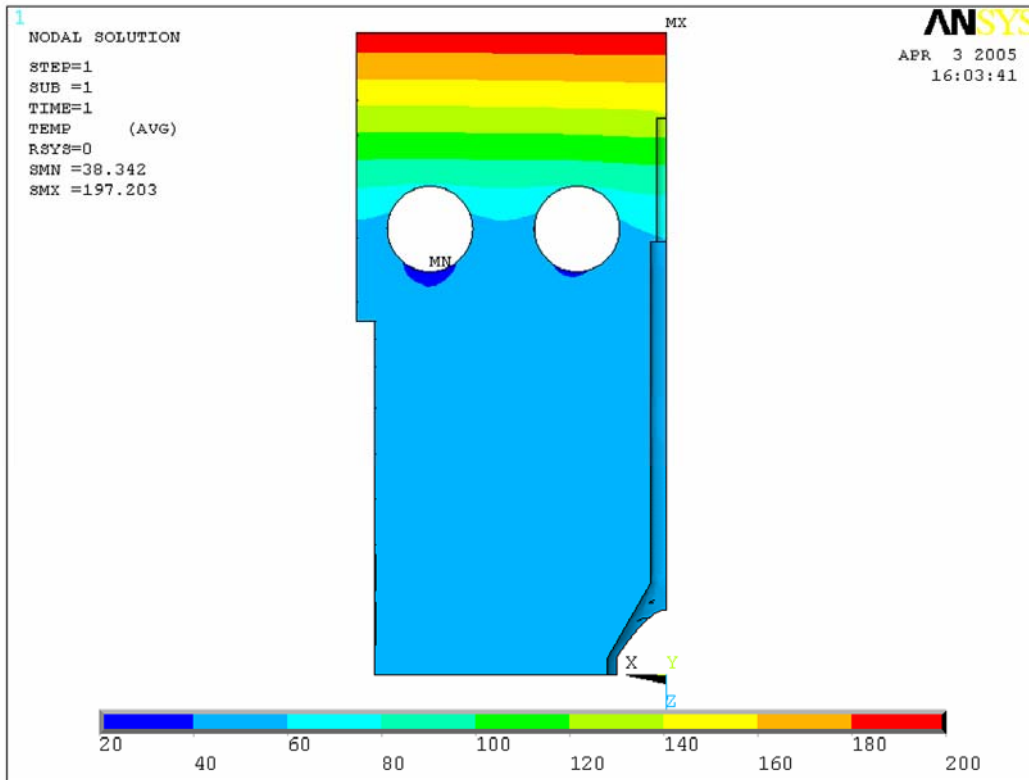


Figure 22: Temperature profile of Case 3 at 800mm

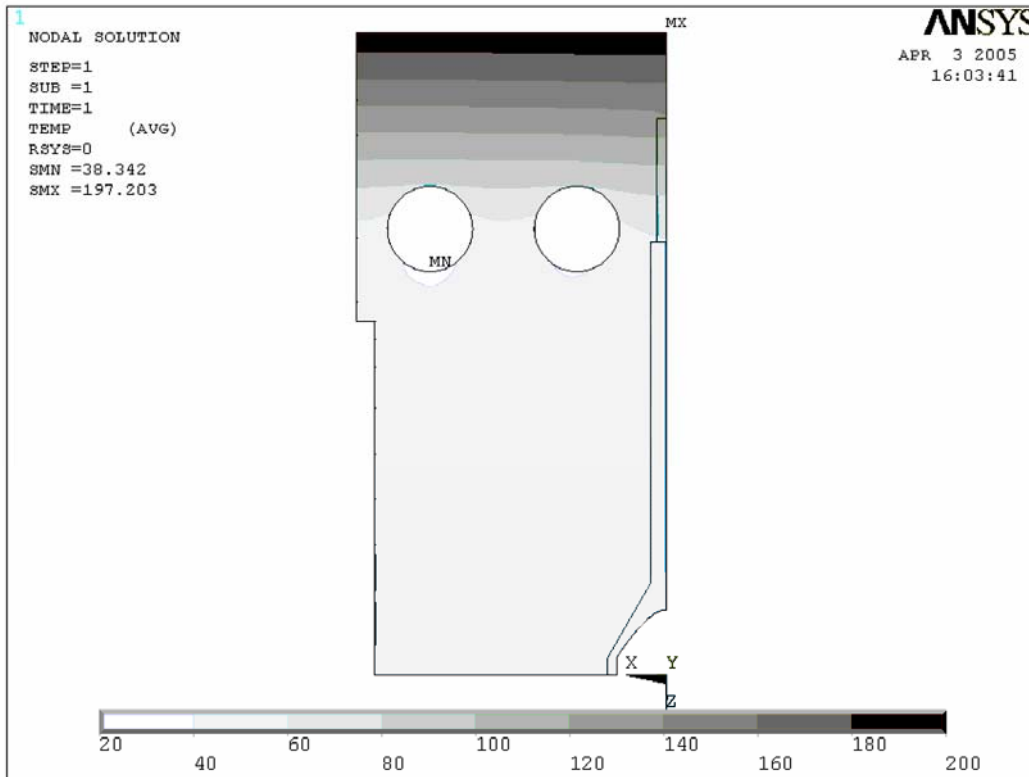


Figure 23: Greyscale of Temperature plot of Case 3 at 800mm

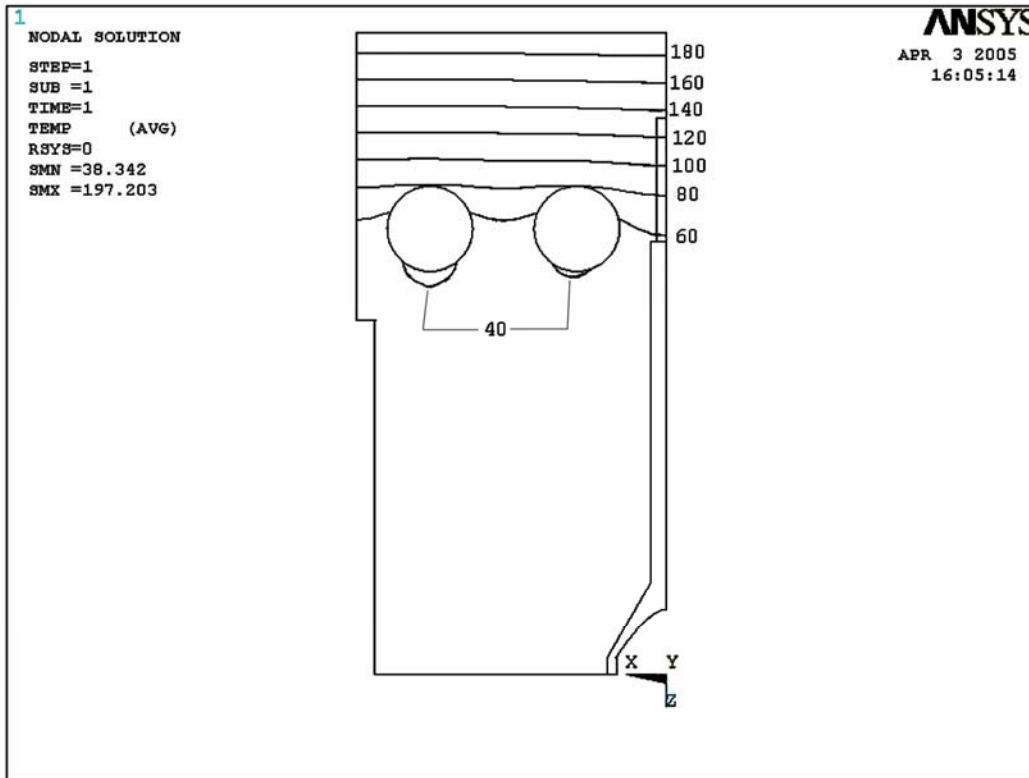


Figure 24: Isoline Plot of Temperature of Case 3 at 800mm

The maximum temperature found was 197.203°C, in a similar position as before. The minimum was found to be 38.342°C.

As before, a better understanding of the temperature profile can be seen by looking at the temperature profile of the top surface alone, shown in Figure 25.

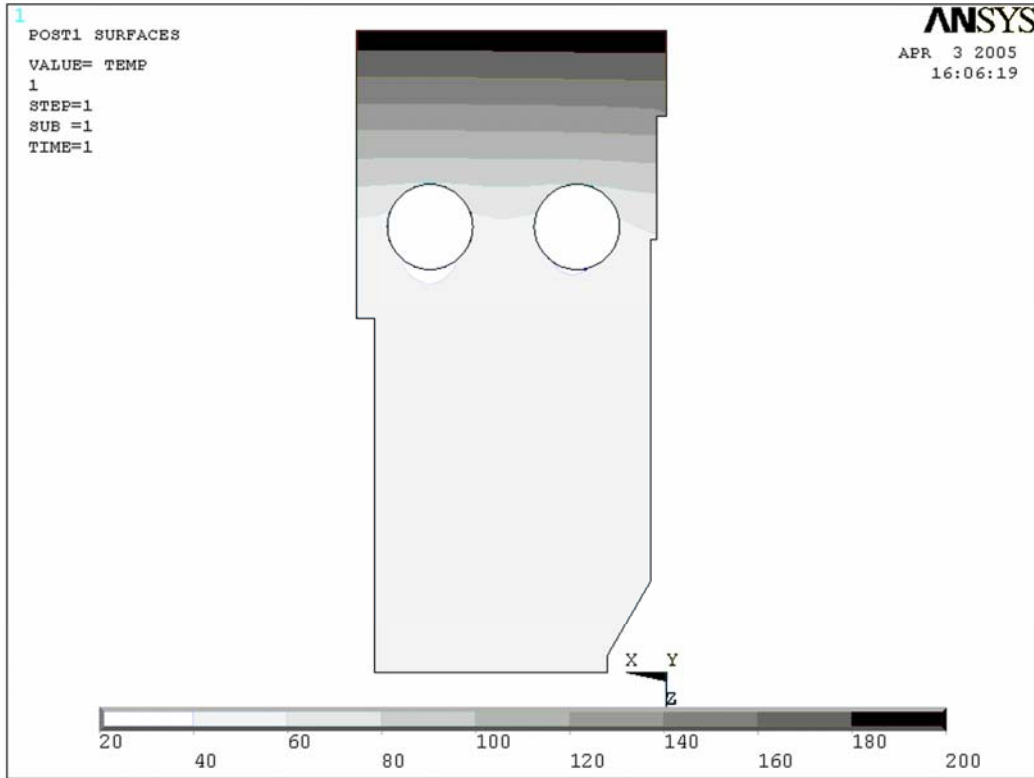


Figure 25: Temperature profile through centre of section in Case 3 at 800mm

Comparison of Cases 1 - 3

It can be seen that the previous fourteen figures do not provide a detailed view of what is occurring in the different Cases so the following graphs show the temperature gradients along certain paths within the model. Figures 26, 27 and 28 are the graphs of each of the three different cases. Figure 29 shows the position of the paths within the domains of all the cases and the positions of the tabulated values.

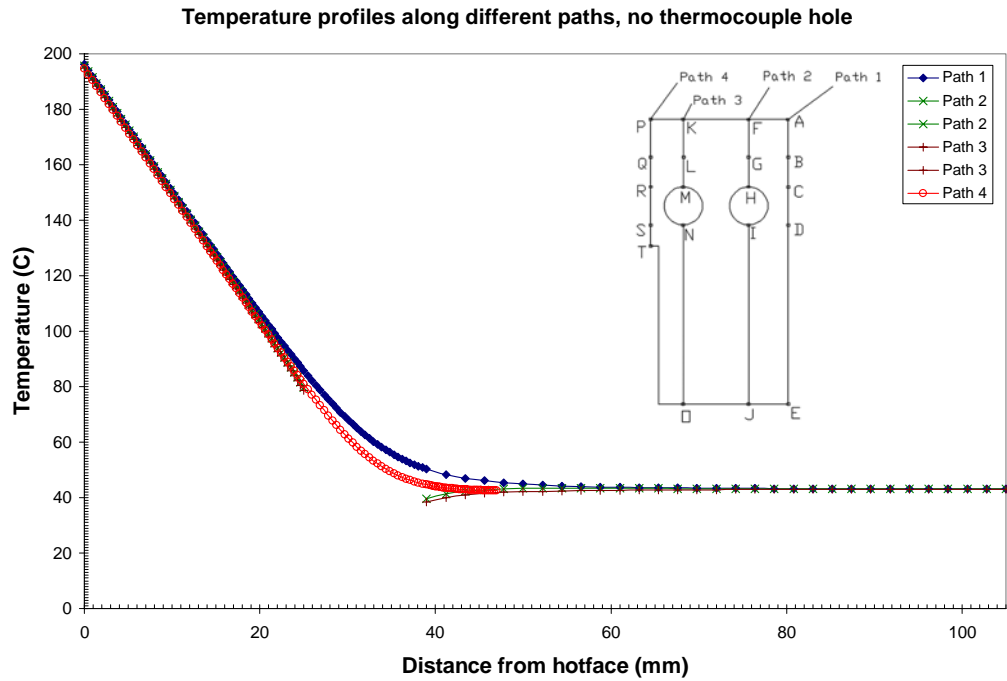


Figure 26: Temperature gradients of different paths within Case 1 at 800mm, no thermocouple hole

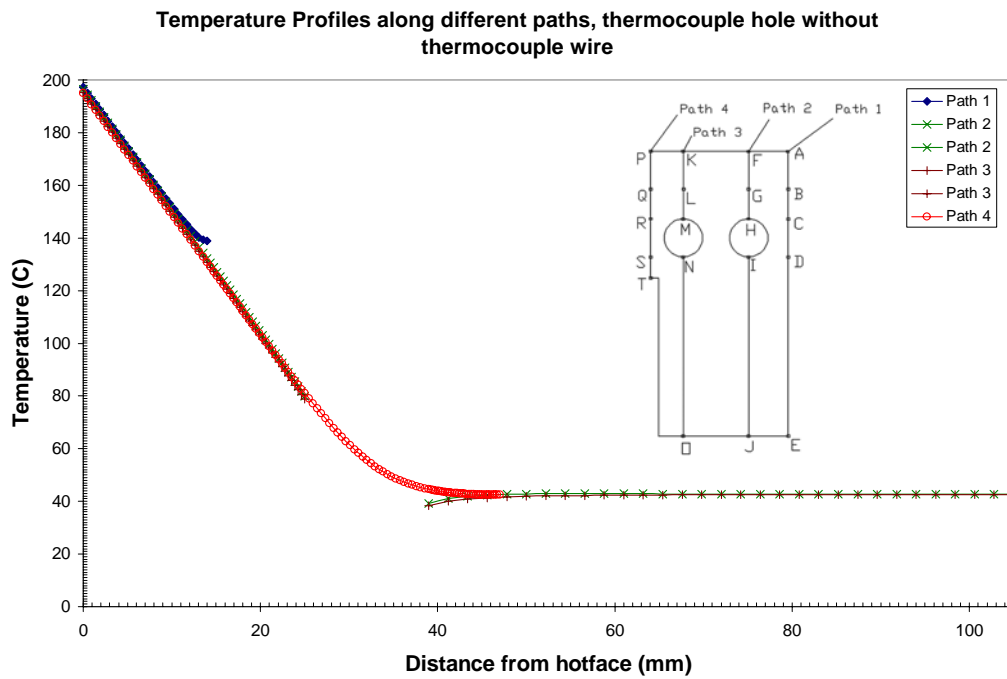


Figure 27: Temperature gradients along different paths within Case 2 at 800mm, thermocouple hole

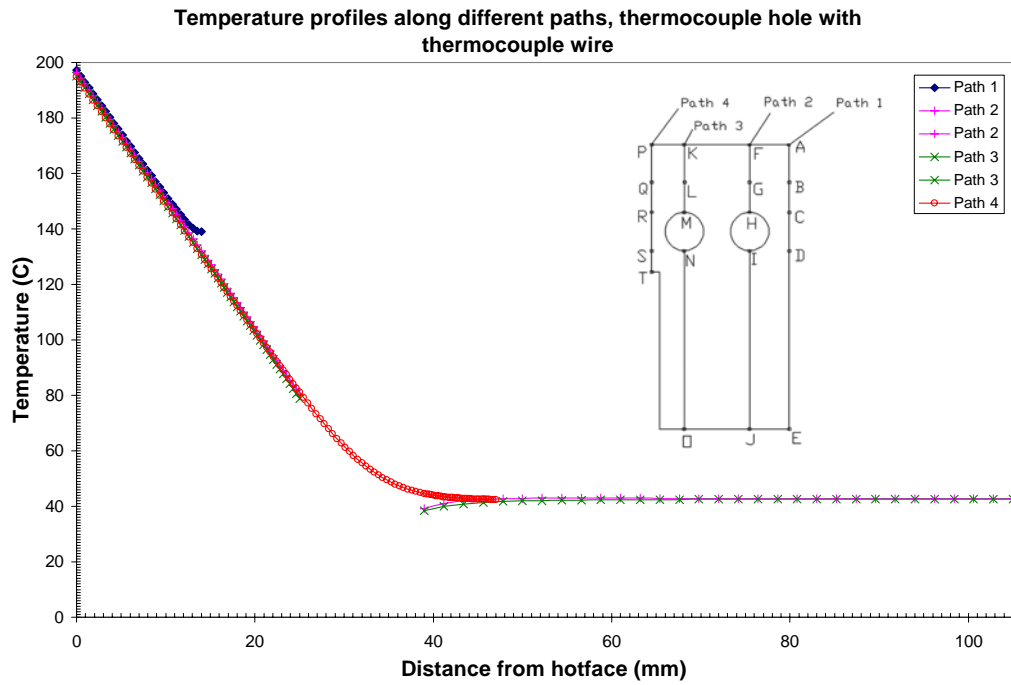


Figure 28: Temperature gradients along different paths within Case 3 at 800mm, thermocouple hole and thermocouple wire

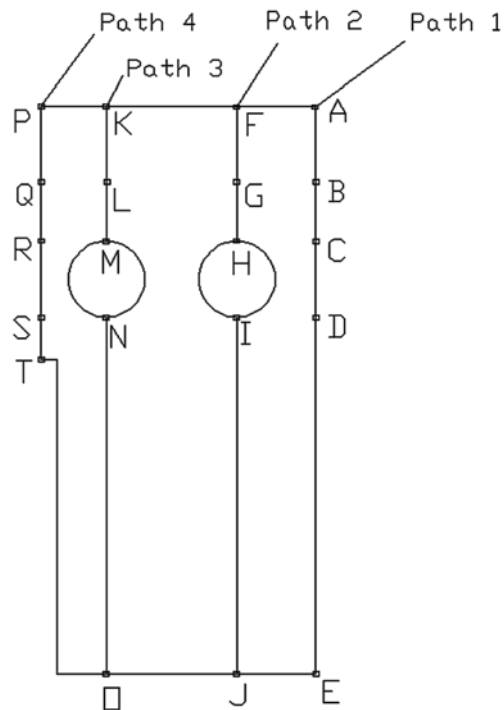


Figure 29: Diagram showing the locations of the paths on the models

Table 6: Results from key points on Cases 1 – 3 at 800mm

No thermocouple hole							
Path 6	Temp	Path 4	Temp	Path 2	Temp	Path 1	Temp
P	194.7	K	194.81	F	195.74	A	196.17
Q	130.47	L	130.45	G	131.58	B	132.7
R	80.996	M	78.671	H	79.693	C	85.797
S	44.671	N	38.438	I	39.563	D	50.294
T	42.591	O	43.017	J	43.102	E	43.128

Thermocouple hole no conduction							
Path 6	Temp	Path 4	Temp	Path 2	Temp	Path 1	Temp
P	194.95	K	195.11	F	196.45	A	197.21
Q	130.67	L	130.68	G	132.17	B	138.95
R	81.093	M	78.787	H	79.974	C	N/A
S	44.589	N	38.345	I	39.299	D	N/A
T	42.46	O	42.638	J	42.697	E	N/A

Thermocouple hole conduction by wire							
Path 6	Temp	Path 4	Temp	Path 2	Temp	Path 1	Temp
P	194.95	K	195.11	F	196.45	A	197.21
Q	130.67	L	130.68	G	132.17	B	138.95
R	81.093	M	78.787	H	79.974	C	N/A
S	44.589	N	38.345	I	39.299	D	N/A
T	42.46	O	42.638	J	42.697	E	N/A

As can be seen Path 1 is shorter on the last two graphs due to the design of the domains, the presence of the thermocouple hole cuts the path short at 14mm from the hot face. This is as expected and allows easy investigation of the temperature at the bottom of the thermocouple hole. For easier comparison of the three simulations below in Figure 30 is a graph showing the temperature gradients of Path 1 of all the three cases.

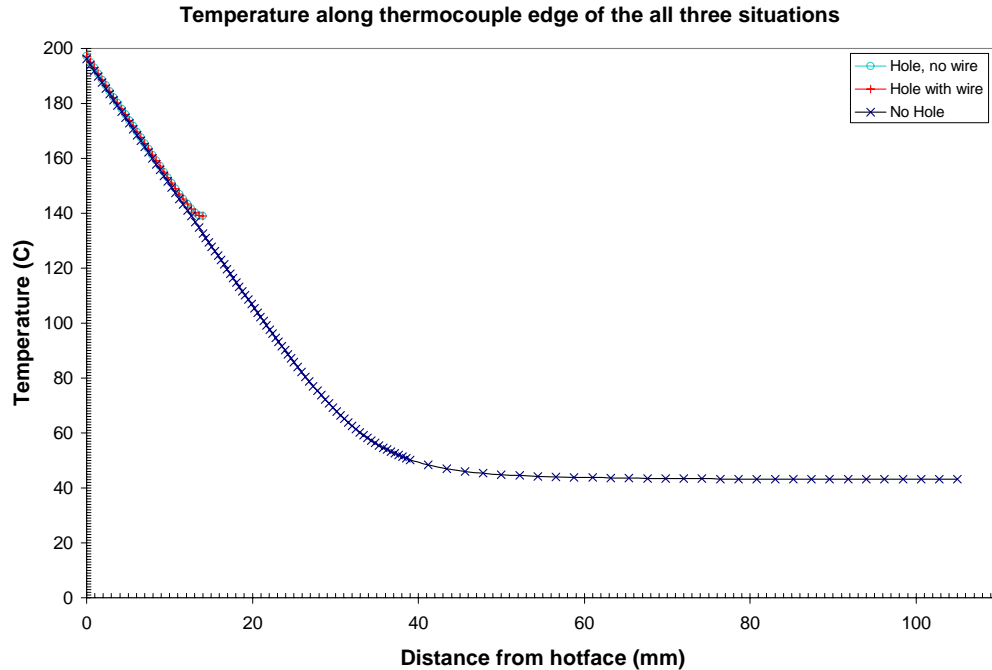


Figure 30: Graph of Path 1 of Cases 1-3

As can be seen the temperature estimated at the position of the thermocouple increases when the thermocouple hole is included. In Case 1, without the thermocouple hole, the temperature was estimated to be 132.7°C. In Case 2 and 3 the temperature was found to be 138.95°C for both cases.

Comparison of Case 2 at 110mm, 400mm and 800mm below the meniscus

This data allows a better understanding of what is occurring within the mould. It can also be used to develop offset values to allow the simpler and quicker CON1D simulation to be used to predict the temperatures at the thermocouples within the mould. At these depths the cooling effect of the thermocouple wire was not included as the amount of heat that is transported away is small and has little effect on the temperature. This was noticed when comparing Cases 2 and 3 at 800mm. Below in Figure 31 is a graph comparing the temperature distributions along Path 1 at the three different depths, 110mm, 400mm and 800mm.

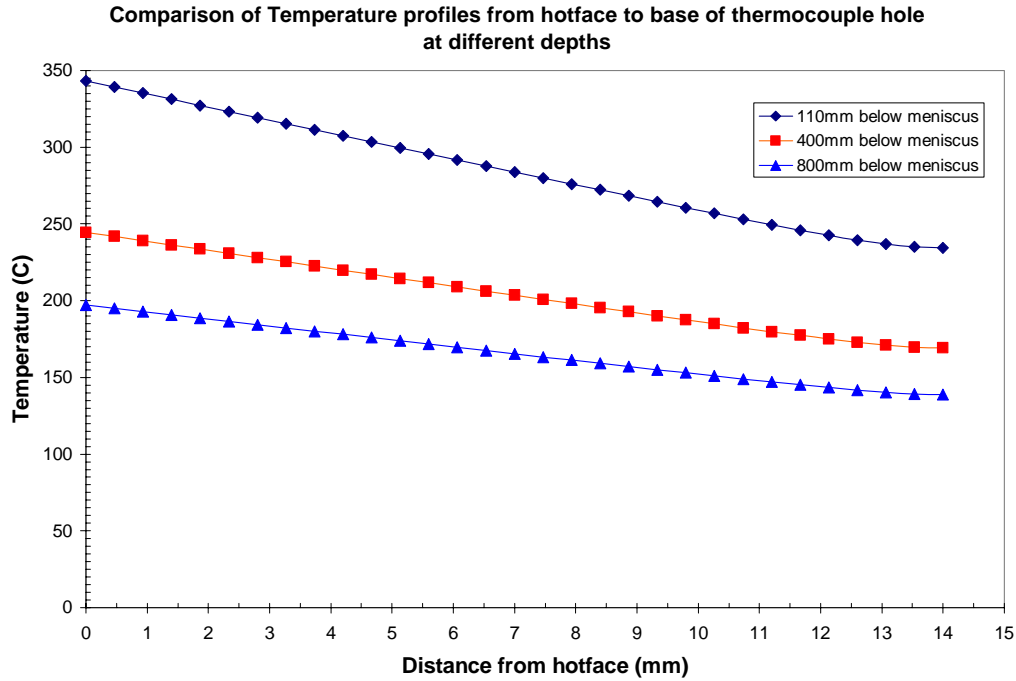


Figure 31: Comparison of Path 1 temperature distributions at different depths (Case 2)

It can be seen that the distributions are similar though as the depth decreases the temperatures obviously increase and the gradients increase due to larger temperature differences between the hot face and the cooling tubes. The temperatures at the base of the thermocouple hole was found to be 234.43°C at 110mm, 169.34°C at 400mm and 139.95°C at 800mm. The maximum hot face temperatures were found to be 343.18°C, 244.6°C and 197.20°C at 110mm, 400mm and 800mm respectively.

In Figure 32 a plot of heat flux against temperature of the hot face is shown. This shows that there is a linear correlation and allows an estimation of hot face temperature if the heat flux can be found or vice-a-versa.

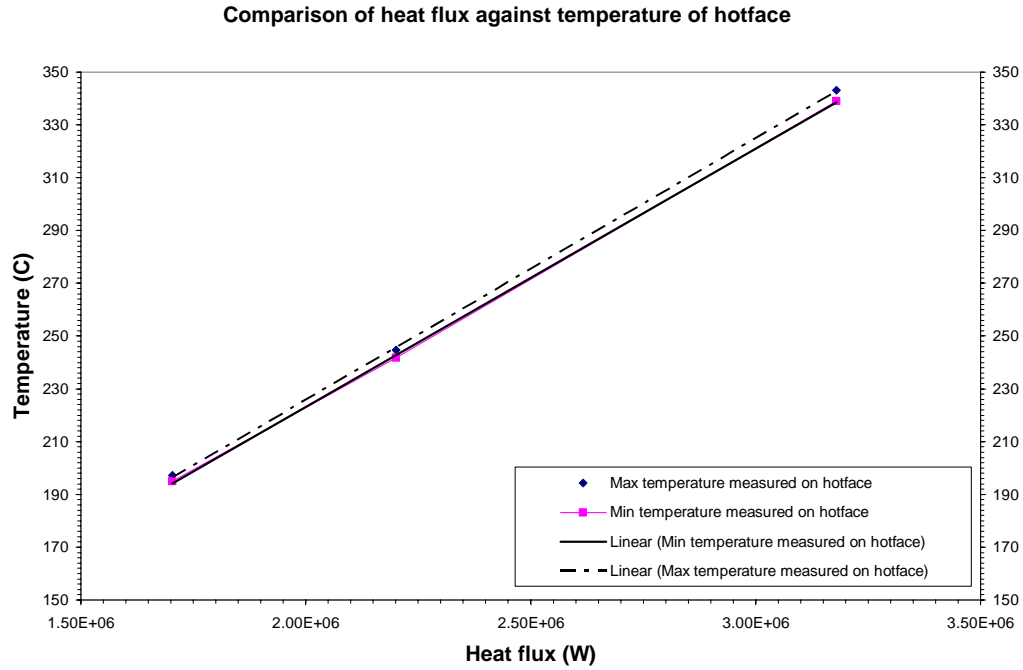


Figure 32: Plot of heat flux from the molten steel compared to hot face temperature
(Case 2 domains)

Comparison of Case 2 and Case 4

The data for Case 4 was compared to Case 2 as both these situations do not contain the thermocouple cooling effect. From the data shown in Figure 33 is a plot along path 1 on the mould, the path from the hot face to the base of the thermocouple hole.

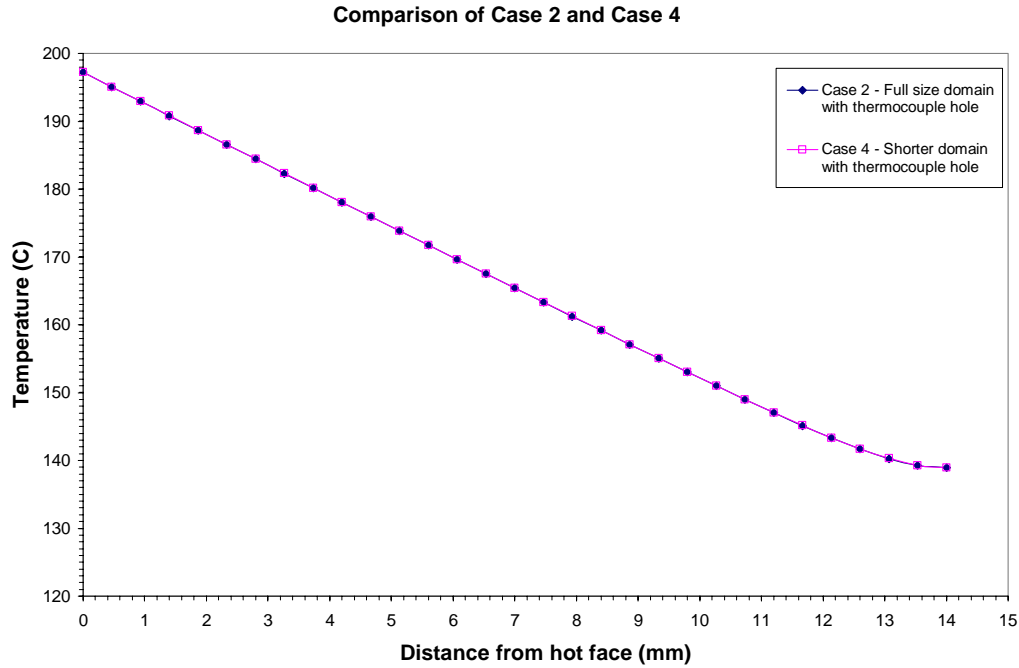


Figure 33: Comparison of Case 2 and Case 4, pathed from hot face to thermocouple hole

It can be seen that there is little variation between the two cases and is consistent with other paths through the mould between the hot face and the cooling tubes. This is expected because the distance of the cooling tubes and thermocouple hole from the hot face remains the same. Even beyond the cooling tubes, the temperature distribution is similar even though the mould ends at a shorter distance from the hot face. This is shown in Figure 34. This means that differences in thermocouple temperatures recorded in the funnel and elsewhere are due to real changes in the heat flux, and not due to the mould design.

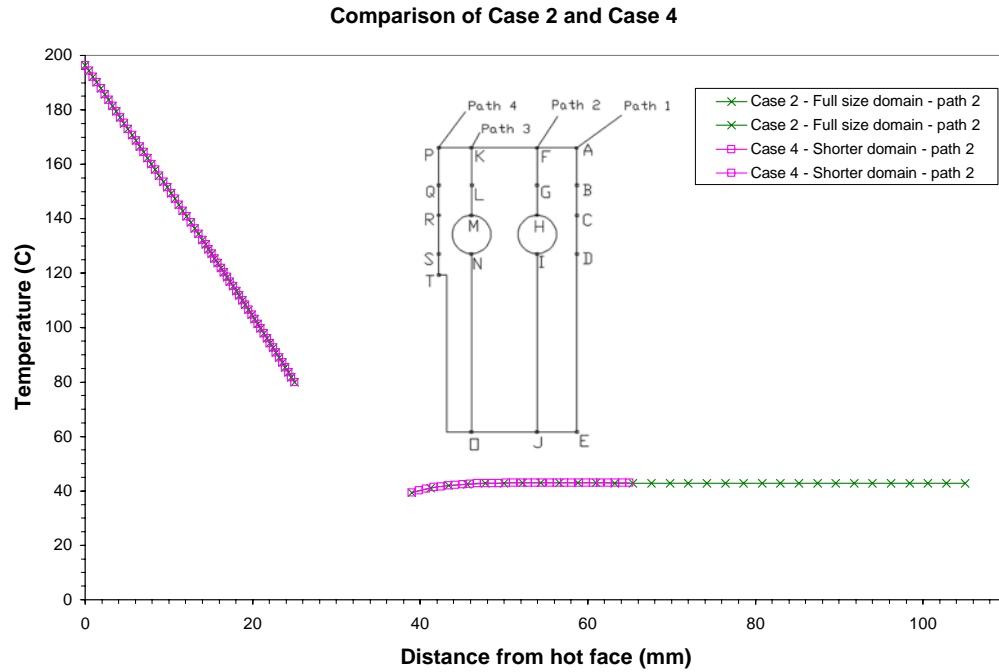


Figure 34: Comparison of temperature profiles for Case 2 and Case 4

Results from Case 5

The purpose of Case 5 was to investigate the temperature profile within the simulation if varying heat flux were being modelled. This is of particular relevance around the meniscus where the heat flux being absorbed by the mould varies significantly. This meniscus area is what has been modelled in Figure 35, 36, 37, 38 and 39. These figures show the domain from several different angles.

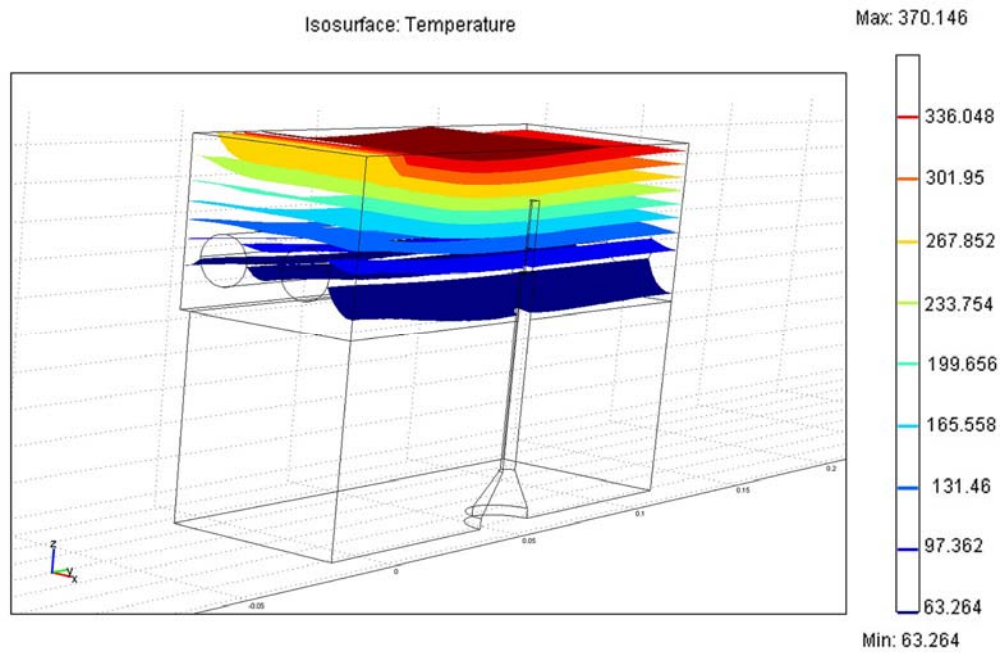


Figure 35: Colour plot of the Case 5 domain showing the temperature profile around the meniscus

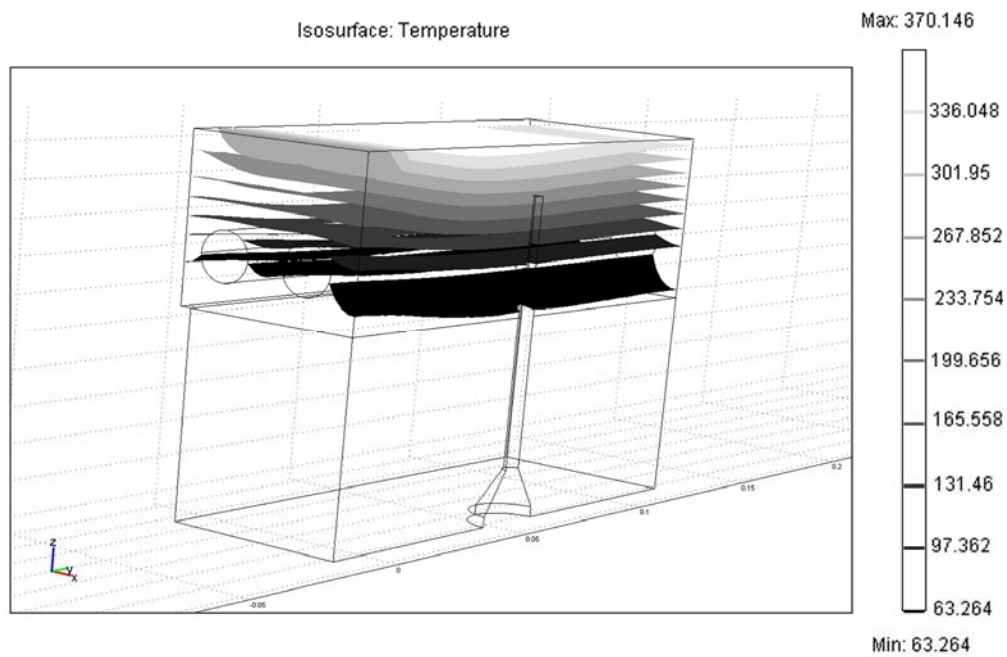


Figure 36: Black and white plot of the Case 5 domain showing the temperature profile around the meniscus

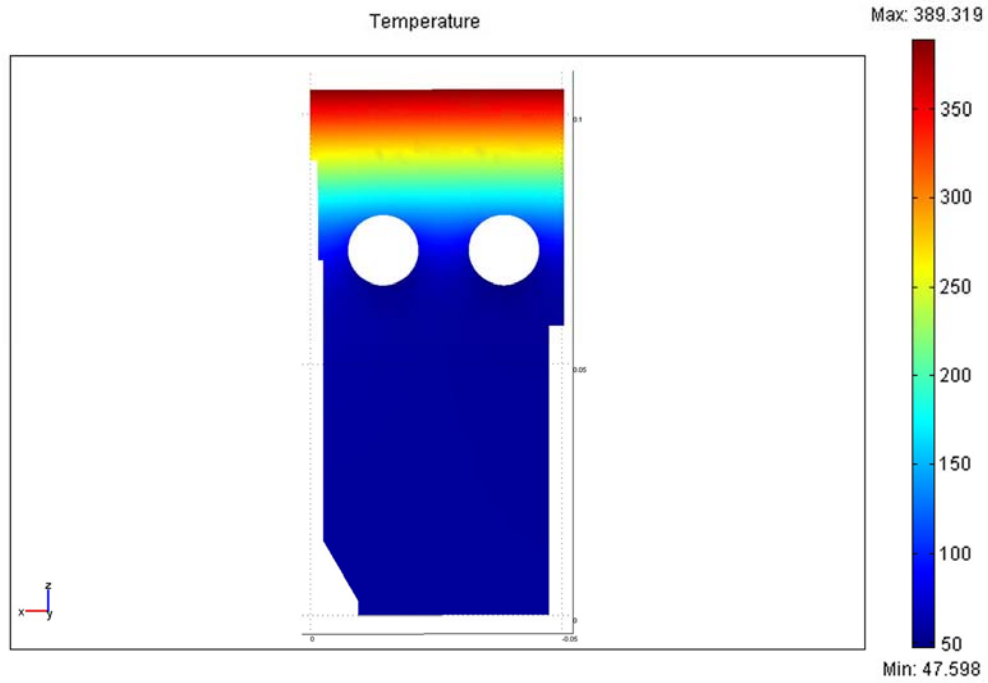


Figure 37: Temperature profile through the plane of the thermocouple

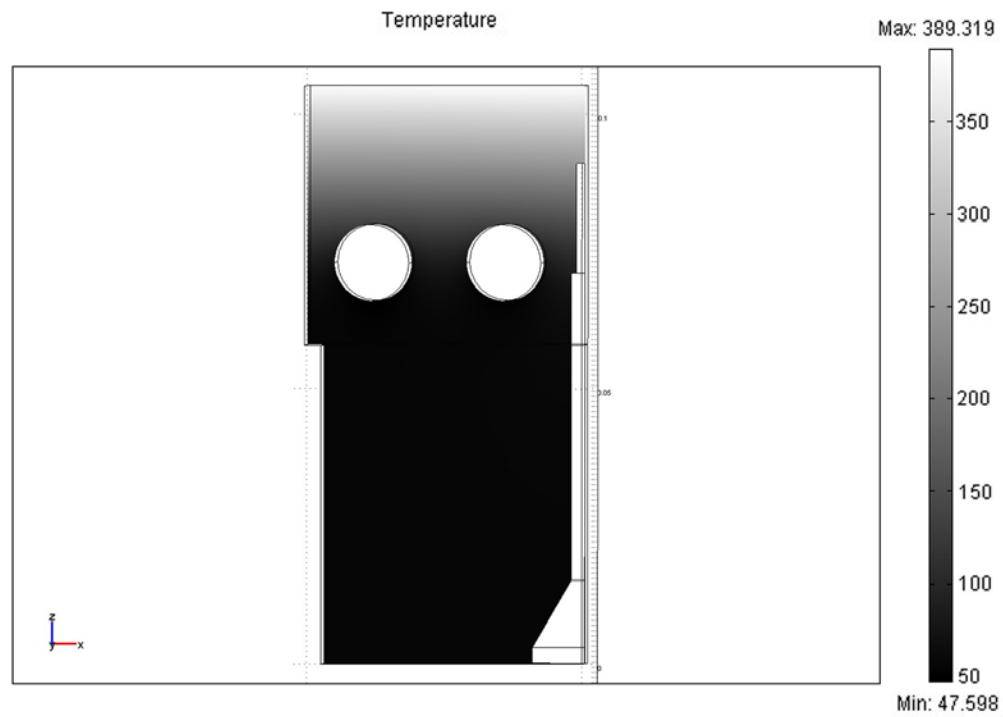


Figure 38: Black and white temperature profile through the plane of the thermocouple

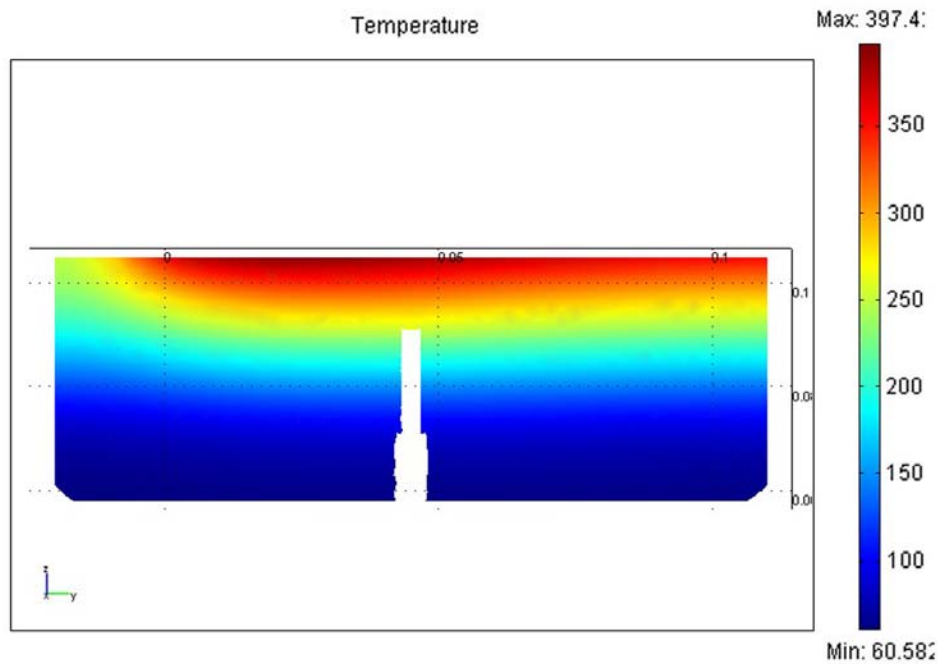


Figure 39: Temperature profile along the thermocouple side of the domain.

As can be seen from these plots the varying heat flux alters the temperature profile as expected though not in any unusual ways. These plots cannot be compared to previous cases as the domain is significantly different however the boundary conditions can be altered so that the thermocouple is placed in the same position as the previous cases. This allows the simulation to be verified and found to be reasonably accurate.

The maximum thermocouple temperatures were found to be 233.3°C, 168.8°C and 136.5°C for the analysed depths of 110mm, 400mm and 800mm below the meniscus. When these are compared to the previous temperatures found of 234.43°C at 110mm, 169.34°C at 400mm and 139.95°C at 800mm it can be seen that there is at least 0.54°C difference though the maximum difference is 3.45°C. This is likely due to an average value being used for the convection coefficient and water temperature in the cooling tubes. Ideally using a similar interpolation method on the tubes as the hot face would have been better but due program errors this was not currently possible but could be achieved in the future.

Another possible reason for this discrepancy is that the position at the base of the thermocouple hole where the temperature was measured for each case was different. There is a small variation in temperature across the base of the thermocouple hole and is shown below in Figures 40 and 41 for a depth of 110mm below the meniscus.

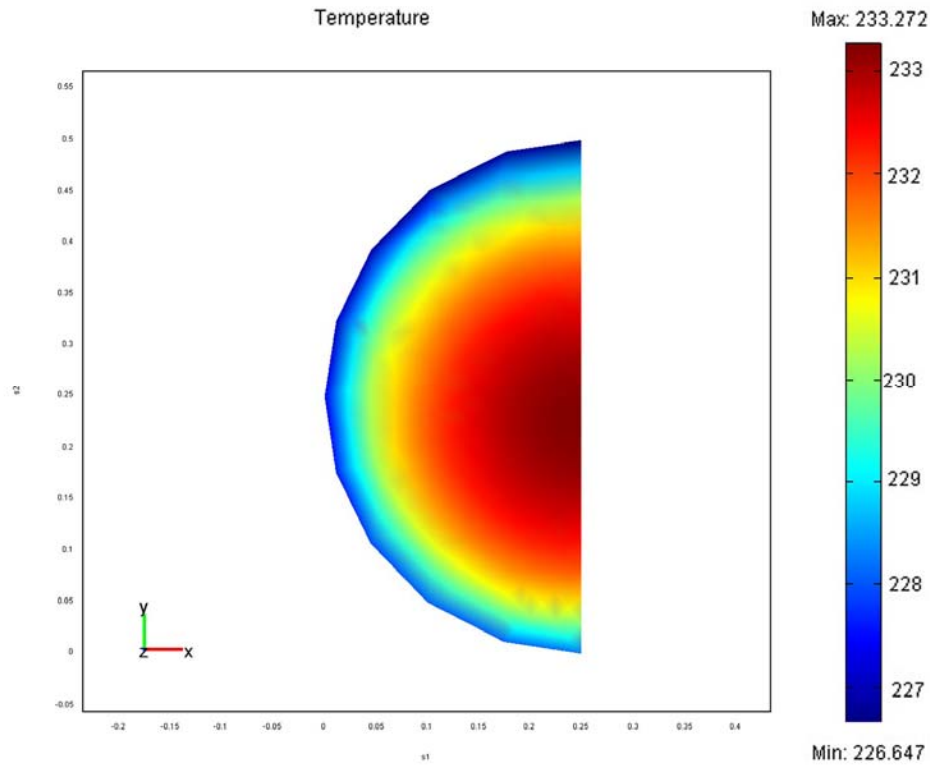


Figure 40: Plot of the temperature profile that exists on the base of thermocouple hole at a depth of 110mm below the meniscus

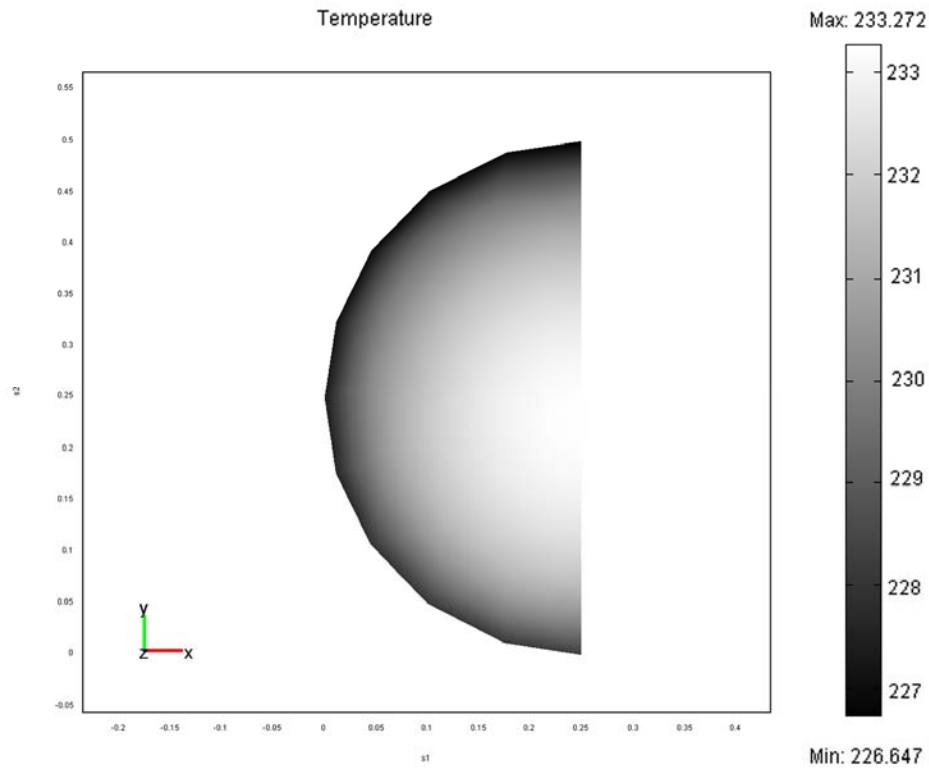


Figure 41: Black and white plot of the temperature profile that exists on the base of thermocouple hole at a depth of 110mm below the meniscus

In this case the temperature varies from 233.3°C to 226.6°C. This difference of 6.7°C is reasonably significant and could be investigated in future studies.

This large domain simulation produces a useful picture of what is occurring and could be used to develop thermocouple temperatures throughout the mould. It shows that the maximum temperature occurs just below the meniscus. The effect of thermocouple hole on the general temperature profile appears to be negligible as there are no noticeable deviations in the isotherms surrounding the thermocouple hole. However under closer inspection there is a slight variation in temperature surrounding the thermocouple hole which can be seen in Figure 40 below.

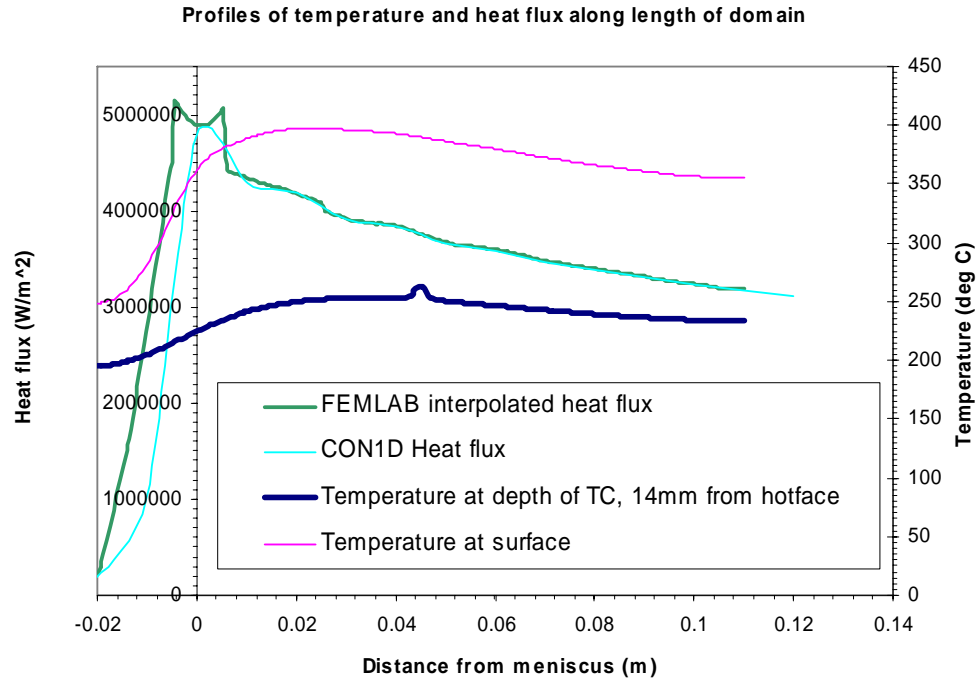


Figure 42: Graph showing the input heat flux and temperatures on the hot face and at the depth of thermocouple throughout the domain.

The input heat flux in this plot is taken from the simulation and is the interpolated values. The interpolation function appears to have produced a slightly idiosyncratic curve surrounding the meniscus though this does not appear to have affected the temperatures. This heat flux curve appears to settle into a relatively straight curve once it is beyond the meniscus.

Model Validation

The model compares well to previously modelled data, using CON1D the input parameter are shown in the appendix as Table 6, where the hot face temperature was estimated by an analytical linear 1-D model from hot face to cooling tubes. The CON1D simulation found the hot face temperature to 194.4°C. In this study the maximum hot face temperature is found to be 194.6°C to 197.20°C.

The results of Cases 2 and 3 at 800mm are similar to those of Case 1 at 800mm, the difference in temperature being explained by the different shape of the

domains used. The new domain has less material to absorb the heat from the hot face creating slightly hotter temperatures. In Case 3 at 800mm the hot face temperature was found to be 194.95°C to 197.20°C. The data developed for Case 2 at 110mm and 400mm appear to agree with the CON1D data like the previous Cases.

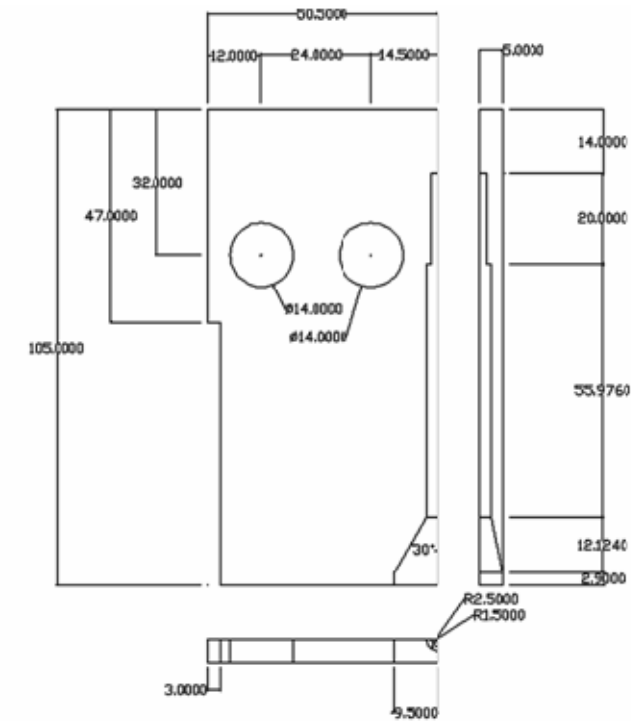
Case 5 was compared with previous cases by simulating the domain at the specific depths. As was mentioned above there is a variation in the thermocouple temperatures between the cases however this can be attributed to several possible factors.

CON1D Calibration

Boundary conditions:

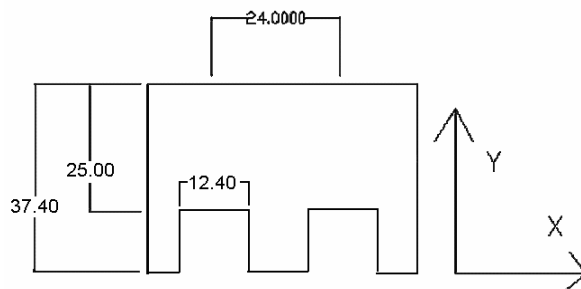
Properties and conditions	ANSYS		CON1D			
Thermal conductivity of copper ($\text{W m}^{-1}\text{K}^{-1}$)	372		372			
Distance of thermocouple from hot face (mm)	14		14 or 12.2			
Remaining faces of model	Perfectly insulated		Perfectly insulated			
Water Velocity in bored holes (m/s)	8.7		8.7			
Conditions at individual depths below meniscus	110 (ANSYS CON1D)		400 (ANSYS CON1D)		800 (ANSYS CON1D)	
Heat Flux (MW m^{-2})	3.18	3.18	2.201	2.201	1.704	1.704
Water tube heat transfer coefficient ($\text{kW m}^{-2}\text{K}^{-2}$)	32.4412	*	34.6691	*	35.7748	*
Water temperature (°C)	21.31	*	25.00	*	28.31	*
* based on Sleicher and Rouse Equation						

ANSYS Case:

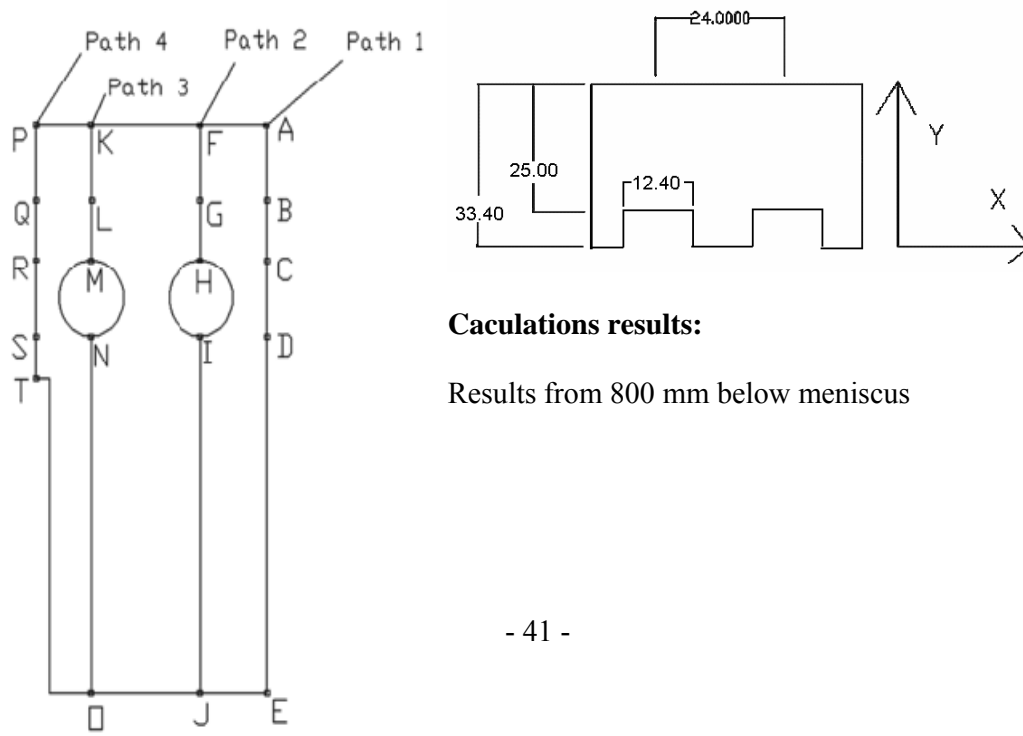


CON1D Cases:

CaseI_WF



CaseIII_WF:



Caculations results:

Results from 800 mm below meniscus

Thermocouple hole no conduction ANSYS							
Path 4	Temp	P 3	Temp	P 2	Temp	P 1	Temp
P	194.95	K	195.11	F	196.45	A	197.21
Q	130.67	L	130.68	G	132.17	B	138.95
R	81.093	M	78.787	H	79.974	C	N/A
S	44.589	N	38.345	I	39.299	D	N/A
T	42.46	O	42.638	J	42.697	E	N/A
CON1D CaseI_WF			CON1D CaseIII_WF				
Hot Face		190.5	Hot Face		195.8		
Cold Face		75.7	Cold Face		81.0		
Distance below meniscus		ANSYS	CON1D CaseIII_WF 14 mm		CON1D CaseIII_WF 12.2 mm		
110		234.43	222.52		237.98		
400		169.34	158.83		169.50		
800		139.95	131.51		139.76		

Thermo couple offset:

Conclusions

From this it can be seen that Case 1 was a reasonable initial approximation however it is better to look into models containing the thermocouple hole as the missing volume has a noticeable effect on the temperature within the mould. This can be seen as the maximum temperature on the hot face increased from 196.17°C to 197.21°C from Case 1 to 2 at 800mm. More importantly the temperature estimated for the thermocouple tip increased from 132.7°C in Case 1 at 800mm to 138.95°C in Case 2 at 800mm. This was caused by the less material in the domain due to the thermocouple hole and is a significant difference which cannot be ignored.

The data comparing the temperatures at different depths can be used to calculate offset values to allow a simple 1-D simulation, like CON1D, to predict the thermocouple temperatures quickly. The values predicted by CON1D will be different from those predicted here however they should be consistently different. This allows the faster running CON1D to be used to predict temperatures if this offset value is accounted for.

The conductive effect of the thermocouple wire was found to be negligible in these simulations, transporting very little heat away from the mould and causing no noticeable change in the temperature at the bottom of the thermocouple hole. The

investigation into effect of air gaps at the thermocouple bead found that this additional thermal resistance can significantly affect the amount of heat transported away by the wire. The heat transported away is reduced further showing that the cooling effect of the thermocouple wires can be neglected. The more important result is the reduction of the temperature present at the thermocouple bead; this shows that the presence of a small air gap can cause a large error in measured temperatures.

The effect of the mould beyond the cooling tubes is found to negligible with no affect on the thermocouple temperature or on the temperature distribution within the mould. This allows a single model to be used for both the funnelled section and the mould edge.

The varying heat flux does cause gross temperature changes within the mould which is as expected. This temperature variation is reasonably linear within the mould at specific distances from the hot face. This linearity breaks down around the meniscus. This section has a rapidly changing heat flux causing rapid temperature rise within the mould making temperature readings within this section to be very sensitive to position. It is recommended to take measurements from a depth below the meniscus and interpolate the hot face temperature around the meniscus from these readings.

These Cases appear to be good estimations of the actual mould. It would be best to conduct parametric studies now to investigate whether this method is reasonable when applied generally. The parametric studies could cover the effect of thermocouple hole size, cooling tube position and size. The meniscus region is the most critical as the most wear occurs here. Further investigation is required to understand more fully the damage effects occurring here.

Finally, CON1D has been calibrated to match the 3-D finite-element model predictions, so long as the mold thickness input to CON1D is fixed at 33.4mm (instead of a range of thicknesses around the of funnel up to 105mm).

The CON1D prediction of thermocouple temperatures is accurate, so long as the thermocouple distance below the hotface is offset by 1.8mm (meaning that TCs in CON1D should be positioned at 12.2 mm below the hotface, which is 1.8mm closer to the hotface than actually occurs in the caster).

Appendix

Table 7: Standard Input Conditions for CON1D simulation

Carbon Content, $C\%$	0.03	%
Liquidus Temperature, T_{liq}	1529	$^{\circ}\text{C}$
Solidus Temperature, T_{sol}	1509	$^{\circ}\text{C}$
Steel Density, ρ_{steel}	7400	kg/m^3
Steel Emissivity, ϵ_{steel}	0.8	-
Fraction Solid for Shell Thickness Location, f_s	0.7	-
Mould Thickness at Top (Outer face, including water channel)	37.4	mm
Mould Outer Face Radius, R_o	0	m
Total Mould Length, Z_{mold_total}	1100	mm
Total Mould Width	1876	mm
Scale thickness at mould cold face (inserts region/ below), d_{scale}	0.02/0.01	mm
Initial Cooling Water Temperature, T_{water}	20	$^{\circ}\text{C}$
Water Channel Geometry, $d_{ch} \times w_{ch} \times L_{ch}$	$12.4 \times 12.4 \times 24$	mm^3
Cooling Water Velocity, V_{water}	8.7	m/s
Mould Conductivity, k_{mold}	360	W/mK
Mould Emissivity, ϵ_{mould}	0.5	-
Mould Powder Solidification Temperature, T_{fsol}	1045	$^{\circ}\text{C}$
Mould Powder Conductivity, k_{solid}/k_{liquid}	1.5/1.5	W/mK
Air Conductivity, k_{air}	0.0599	W/mK
Slag Layer/Mould Resistance, $r_{contact}$	5.0E-9	$\text{m}^2\text{K/W}$
Mould Powder Viscosity at 1300°C , μ_{1300}	1.2	Poise
Exponent for Temperature dependence of Viscosity, n	0.85	-
Slag Density, ρ_{slag}	2500	kg/m^3
Slag Absorption Factor, a	250	m^{-1}
Slag Refractive Index, m	1.5	-
Slag Emissivity, ϵ_{slag}	0.9	-
Mould Powder Consumption Rate, Q_{slag}	0.12	kg/m^2
Empirical solid slag layer speed factor, f_v	0.175	-
Casting Speed, V_c	3.6	m/min
Pour Temperature, T_{pour}	1550	$^{\circ}\text{C}$
Slab Geometry, $W \times N$	1450×90	$\text{mm} \times \text{mm}$
Nozzle Submergence Depth, d_{nozzle}	265	mm
Working Mould Length, Z_{mold}	1100	mm
Oscillation Mark Geometry, $d_{mark} \times w_{mark}$	0.1×1	$\text{mm} \times \text{mm}$
Mould Oscillation Frequency, $freq$	4.67	cpm
Oscillation Stroke, $stroke$	6	mm
Time Step, dt	0.002	s
Mesh Size, dx	0.5	mm

References

1. Metallurgical and Materials Transactions B, Vol. 34B, No. 5, Oct., 2003, pp. 685-705.
2. www.ansys.com
3. www.comsol.com

Simulation Conditions	
Thermal conductivity of copper	372 W m ⁻¹ K ⁻¹
Distance of thermocouple from hot face	14mm
Remaining faces of model	Perfectly insulated
Water Velocity in bored holes	8.7 m/s
Depth below meniscus (mm)	800
Heat Flux (MW m ⁻²)	1.704
Water tube heat transfer coefficient (kW m ⁻² K ⁻²)	35.7748
Water temperature (°C)	28.31